



UNESP – Universidade Estadual Paulista  
“Júlio de Mesquita Filho”  
Faculdade de Odontologia de Araraquara



Ana Lúcia Roselino Ribeiro

**Corrosão e tribocorrosão de novas ligas  
Ti35Nb5Zr e Ti35Nb10Zr em saliva artificial**

**Araraquara**

**2012**



UNESP – Universidade Estadual Paulista  
“Júlio de Mesquita Filho”  
Faculdade de Odontologia de Araraquara



Ana Lúcia Roselino Ribeiro

## **Corrosão e tribocorrosão de novas ligas Ti35Nb5Zr e Ti35Nb10Zr em saliva artificial**

Tese apresentada ao Programa de Pós-Graduação em Odontologia - Área de Periodontia, da Faculdade de Odontologia de Araraquara, Universidade Estadual Paulista “Júlio de Mesquita Filho”, para obtenção do título de Doutor em Odontologia.

Orientador: Prof. Dr. Luís Geraldo Vaz  
Coorientador: Prof. Dr. Luís Augusto Sousa Marques da Rocha

**Araraquara**

**2012**

Ribeiro, Ana Lúcia Roselino

Corrosão e tribocorrosão de novas ligas de Ti35Nb5Zr e Ti35Nb10Zr em saliva artificial / Ana Lúcia Roselino Ribeiro. - Araraquara: [s.n.], 2012.

118 f. ; 30 cm.

Tese (Doutorado) – Universidade Estadual Paulista, Faculdade de Odontologia

Orientador: Prof. Dr. Luís Geraldo Vaz

Co-orientador: Prof. Dr. Luís Augusto Sousa Marques da Rocha

1. Ligas de titânio\* 2. Implantes dentários 3. Corrosão  
4. Tribocorrosão\* I. Título

Ficha catalográfica elaborada pela Bibliotecária Marley C. Chiusoli Montagnoli, CRB-8/5646  
Serviço Técnico de Biblioteca e Documentação da Faculdade de Odontologia de Araraquara / UNESP

\* Descritores da área de Química, descritos no Bibliodata

Ana Lúcia Roselino Ribeiro

**Corrosão e tribocorrosão de novas ligas  
Ti35Nb5Zr e Ti35Nb10Zr em saliva artificial**

COMISSÃO JULGADORA

TESE PARA OBTENÇÃO DO GRAU DE DOUTOR

Presidente e Orientador: Prof. Dr. Luís Geraldo Vaz

2º Examinador: Prof. Dr. Joni Augusto Cirelli

3º Examinador: Profa. Dra. Maria da Glória Chiarello de Mattos

4º Examinador: Prof. Dr. Danilo Luiz Flumignan

5º Examinador: Prof. Dr. Márcio Luiz dos Santos

Araraquara, 28 de março de 2012.

## **DADOS CURRICULARES**

Ana Lúcia Roselino Ribeiro

Nascimento: 19/11/1981 – Ribeirão Preto/SP

Filiação: José Eduardo Ribeiro  
Ana Maria Ferreira Roselino

2001/2004 **Graduação em Odontologia**  
Faculdade de Odontologia de Araraquara – UNESP

2003/2004 **Estágio de Iniciação Científica na Disciplina de Materiais Dentários**  
Orientador: Prof. Dr. Luís Geraldo Vaz  
Faculdade de Odontologia de Araraquara – UNESP

2004 **Bolsista FAPESP de Iniciação Científica (04/00497-3)**  
Orientador: Prof. Dr. Luís Geraldo Vaz

2005/2006 **Estágio na Disciplina de Materiais Dentários**  
Orientador: Prof. Dr. Luís Geraldo Vaz  
**Estágio de Atualização na Disciplina de Clínica Integrada**  
Orientador: Prof. Dr. Oscar Fernando Muñoz-Chávez  
Faculdade de Odontologia de Araraquara – UNESP

- 2005/2006 **Curso de Aperfeiçoamento em Reabilitação Oral e Clínica Integrada**  
Associação Paulista de Cirurgiões Dentistas/Escola de Aperfeiçoamento Profissional – APCD/EAP (Regional Araraquara)
- 2006/2008 **Pós-Graduação em Odontologia – Nível Mestrado**  
Área de Concentração Periodontia  
Faculdade de Odontologia de Araraquara – UNESP  
Bolsista CAPES  
APQ/ FAPESP (2006/06253-4)
- 2007/2009 **Especialização em Periodontia**  
Fundação Araraquarense de Ensino a Pesquisa em Odontologia – FAEPO
- 2008/2012 **Pós-Graduação em Odontologia – Nível Doutorado**  
Área de Concentração Periodontia  
Faculdade de Odontologia de Araraquara – UNESP  
Bolsista CAPES  
APQ/ FAPESP (2007/07090-4)
- 2010/2011 **Estágio de Doutorado Sanduíche**  
Faculdade de Engenharia Mecânica  
CT2M - Centre for Mechanics and Materials Technologies  
Universidade do Minho, Guimarães - Portugal  
Bolsista CAPES (1424-10-6)

## DEDICATÓRIA

À minha mãe, Ana Maria, pelo amor, exemplo de vida, apoio e confiança, que me fazem seguir este caminho com coragem e determinação e por estar sempre presente em todos os momentos da minha vida.

Ao meu pai, José Eduardo, pelo incentivo aos estudos e exemplo de determinação.

Ao meu irmão, Dudu, que sempre esteve comigo, me defendendo, apoiando e alegrando minha vida.

A minha sobrinha, Betina, por alegrar e unir a família.

## **AGRADECIMENTOS**

Ao Prof. Dr. Luís Geraldo Vaz, pela orientação, pela disponibilidade, pela confiança e por toda a atenção dedicada durante esses nove anos de convivência acadêmica.

Ao Prof. Dr. Luís Augusto Sousa Marques da Rocha, pela orientação e disponibilidade, por todo conhecimento científico ensinado e pela oportunidade ímpar em desenvolver esse trabalho em seu laboratório.

À Faculdade de Odontologia de Araraquara – UNESP, em nome do Ilmo. Sr. Diretor, Prof. Dr. José Cláudio Martins Segalla, e da Ilma. Sra. Vice-Diretora, Prof.<sup>a</sup> Dr.<sup>a</sup> Andreia Affonso Barretto Montandon, pela oportunidade de ganho profissional.,

À Faculdade de Engenharia Mecânica e ao CT2M – Universidade do Minho, em nome de todas as pessoas que me ajudaram na realização desse trabalho, coorientador, professores, funcionários e alunos, pela oportunidade de enriquecimento profissional.

À CAPES, pela concessão da Bolsa de estudos regular no país e pela Bolsa de estudos PDEE, em Portugal.

À FAPESP, pelo financiamento concedido à solicitação Auxílio à Pesquisa.

Aos professores da Disciplina de Periodontia, Faculdade de Odontologia de Araraquara - UNESP: Prof. Dr. José Eduardo, Prof.<sup>a</sup> Dr.<sup>a</sup> Silvana, Prof. Dr. Joni, Prof.<sup>a</sup> Dr.<sup>a</sup> Adriana, Prof. Dr. Élcio, Prof. Dr. Carlos, Prof. Dr. Egbert e Prof. Dr. Ricardo, pelos conhecimentos adquiridos.



Aos professores da Disciplina de Materiais Odontológicos e Prótese, Faculdade de Odontologia de Araraquara - UNESP: Prof. Dr. Carlos Cruz, Prof. Dr. Gelson, Prof.<sup>a</sup> Dr.<sup>a</sup> Renata, pela agradável convivência e apoio.

A todos os funcionários do Departamento de Diagnóstico e Cirurgia, da Faculdade de Odontologia de Araraquara - UNESP, em nome dos funcionários Regina Lúcia, Zezé, Ester e D. Maria, pelo carinho a mim dispensado.

A todos os funcionários do Departamento de Materiais Odontológicos e Prótese, da Faculdade de Odontologia de Araraquara – UNESP, em especial a Marta, Sílvia e Adelaides pelo convívio agradável e disponibilidade em me ajudar.

A todos os funcionários da Faculdade de Engenharia Mecânica da Universidade do Minho, em especial a dona Luisa, Silvia, Miguel, Vitor e Sérgio, pelos serviços prestados, pelo convívio agradável e disponibilidade em me ajudar.

Ao Dr. Danilo Luiz Flumignan, pelo apoio nas análises químicas realizadas no Cempeqc - IQ – Unesp.

Ao Dr. Peter Hammer, pelas análises de XPS realizadas no IQ – UNESP.

Aos funcionários da Biblioteca da Faculdade de Odontologia de Araraquara – UNESP, em especial a Ceres, pela atenção e disponibilidade em nos auxiliar.

Aos funcionários da Seção de Pós Graduação, da Faculdade de Odontologia de Araraquara – UNESP, em especial a Mara, pela dedicação e atenção em nos auxiliar.

A todos os funcionários dos laboratórios em que passei para realizar este trabalho, pela disposição e ensinamentos.

A todos os alunos de Pós Graduação em Odontologia, em nome dos meus amigos companheiros de turma de Doutorado: Andrés, Humberto, Marina, Roberta, Rodrigo, Rubens, Sabrina, Shelon, Yeon e Wagner, pela amizade, pelas experiências compartilhadas, pela cumplicidade e pelos bons momentos de convivência durante todo o curso. Especialmente aos amigos do Euro-Perio-Foar-2010!

A toda equipe do professor Geraldo: Cássia, Henrique, Laiza, Marcela, Roberto e Sarah pela amizade e pelos conhecimentos compartilhados. Especialmente à Cássia, pelo convívio, pela visita em Portugal, por compartilhar todos os momentos dessa jornada, sempre disposta a me ajudar, até emprestando sua casa para eu morar.

A toda equipe do laboratório de Portugal: Prof. Luís, Profa Ana Maria, Prof. José Gomes, Alexandra, Angela, Catarina, Eva, Fatih, Fernando, Helena, Jefferson, Maria João, Sónia Costa, Sónia Ferreira, Tuan e Vicente, por toda a ajuda, companheirismo e amizade do primeiro ao último dia que estive em Guimarães. Espero que a amizade e troca de conhecimentos continue.

Ao casal Luís e Ana e família, pela boa convivência e por ter me recebido tão bem em Portugal.

Aos amigos Vimaranenses, Bracarense, Covilhanense e Ronfense, por tudo e mais um pouco... Fernando, Helena, Jefferson, Maria João e Sónia, adorei ter-vos conhecido! Vocês, além de fixes, são giríssimos!

Aos amigos de Araraquara, Ribeirão Preto e Picinguaba, que são muitos, pela felicidade!!!

A todos os colegas e amigos de Pós-Graduação, da Faculdade de Odontologia de Araraquara – UNESP, pela convivência agradável e oportunidade de aprendizado.

À minha querida mãe, por sempre me incentivar, pela ajuda em Portugal no primeiro mês in loco e depois pelo skype, pelo apoio emocional e financeiro, e também pelos sonhos compartilhados!

Ao meu irmão Dudu e minha cunhada Dani, por todo carinho, atenção e torcida, e em especial pelo nascimento da Betina.

Ao Claudinho, pelo amor e companheirismo, por aguentar meu estresse e neuras, pela longa visita em Portugal, pelas viagens, por tudo que vivemos juntos.

À toda minha família e amigos, que sempre torceram por mim; especialmente à minha avó Sylvia (*in memoriam*), por sempre ter incentivado à leitura e exemplo de mulher e ao meu avô Ruy (*in memoriam*), pelo exemplo de carreira acadêmica.

A todos aqueles que, direta ou indiretamente, contribuíram para a realização deste trabalho.

*Picinguaba...*

*Sunrising brings peace*

*The ocean finishes into the sky*

*White and fine powder sand*

*Falling down through my fingers*

*My heart finally stops to cry*

*Sunsetting brings peace*

*The ocean is so far from the sky*

*Star lights, night, people alive*

*Tears leaving my eyes*

*Waiting for tomorrow's sunshine*

## SUMÁRIO

<b>Resumo</b> .....	11
<b>Abstract</b> .....	12
<b>Introdução</b> .....	13
<b>Capítulo 1</b>	
Are new TiNbZr alloys potential substitutes for the Ti6Al4V alloy for dental applications? A corrosion behaviour view.....	23
<b>Capítulo 2</b>	
On the tribocorrosion of new Ti35Nb5Zr and Ti35Nb10Zr alloys for dental applications: passive film vs. bulk behaviour.....	60
<b>Considerações finais</b> .....	95
<b>Conclusão geral</b> .....	99
<b>Referências</b> .....	100
<b>Apêndice</b> .....	110

Ribeiro ALR. Corrosão e tribocorrosão de novas ligas Ti35Nb5Zr e Ti35Nb10Zr em saliva artificial. [Tese de Doutorado]. Araraquara: Faculdade de Odontologia da UNESP; 2012.

## Resumo

O sucesso dos implantes dentários em longo período depende da interação do biomaterial com o ambiente bucal, a qual envolve reações eletroquímicas, resistência mecânica e desgaste mecânico. Com o intuito de melhorar a resistência mecânica e à corrosão do titânio (Ti), elementos de liga são adicionados, sendo a liga Ti6Al4V a mais comum. Porém, o vanádio e o alumínio são considerados potencialmente tóxicos. Portanto, nos últimos anos, esforços vêm sendo feitos para o desenvolvimento de novas ligas de Ti ultra resistentes e biocompatíveis, a partir do sistema TiNbZr. Assim, o objetivo desse trabalho foi avaliar a corrosão e tribocorrosão das novas ligas Ti35Nb5Zr e Ti35Nb10Zr em saliva artificial a 37°C comparadas à liga comercial Ti6Al4V. Testes de potencial de circuito aberto com o tempo ( $E_{corr}$ ) e espectroscopia de impedância eletroquímica (EIS) foram realizados em função do tempo (0-216h). Testes de tribocorrosão em função de cargas aplicadas (50mN-1N) foram realizados tanto em  $E_{corr}$  como em potencial anódico aplicado. Como resultados, todas as ligas exibiram aumento de  $E_{corr}$  com o tempo, indicando crescimento e estabilização do filme passivo. Os experimentos de EIS indicaram que a liga Ti35Nb10Zr possui resistência à corrosão ligeiramente maior que a liga Ti6Al4V, assim como melhor comportamento tribocorrosivo quando realizado com baixa carga. Portanto, o filme passivo formado na liga Ti35Nb10Zr possui melhor resistência à corrosão e ao desgaste devido à presença de Nb<sub>2</sub>O<sub>5</sub> e ZrO<sub>2</sub>. Porém, o metal base da liga Ti6Al4V apresentou menor desgaste mecânico. Concluindo, a liga de Ti35Nb10Zr é candidata promissora a ser utilizada na fabricação de conjuntos implantes-componentes protéticos.

Palavras-chave: Ligas de titânio; implantes dentários; corrosão; tribocorrosão.

Ribeiro ALR. Corrosion and tribocorrosion of new Ti35Nb5Zr and Ti35Nb10Zr in artificial saliva. [Tese de Doutorado]. Araraquara: Faculdade de Odontologia da UNESP; 2012.

## **Abstract**

The long-life success of dental implants relies on the interaction between the biomaterial and oral environment, always involving electrochemical reactions, mechanical stresses and mechanical wear. In order to improve the mechanical strength and corrosion resistance of titanium (Ti), alloying elements are added to it, the most common alloy being Ti6Al4V. However, vanadium and aluminum are known to be toxic. Therefore, in last years, efforts are being made towards the development of new high resistant and biocompatible titanium alloys, namely from the TiNbZr system. Therefore, the aim of this work was to assess the corrosion and tribocorrosion behavior of new Ti35Nb5Zr and Ti35Nb10Zr in artificial saliva at 37°C, in comparison with the commercial Ti6Al4V alloy. Open circuit potential ( $E_{corr}$ ) and electrochemical impedance spectroscopy (EIS) experiments were carried in function of time (0-216h). Tribocorrosion tests were performed at different applied loads (50mN to 1N) both at  $E_{corr}$  and anodic applied potential. In general, all alloys exhibited an increase of  $E_{corr}$  with the immersion time, indicating the growth and stabilization of the passive film. The EIS results indicated that Ti35Nb10Zr alloy exhibited slightly better corrosion resistance than Ti6Al4V. Just as better tribocorrosion behavior at low applied loads. Therefore, the passive film formed on Ti35Nb10Zr alloy had better mechanical strength and corrosion resistance due to  $Nb_2O_5$  e  $ZrO_2$ . However, the bulk metal of Ti6Al4V suffered less mechanical wear. Concluding, Ti35Nb10Zr alloy appear as promising candidate for dental implant-abutment sets manufacturing.

Keywords: Titanium alloys; dental implants; corrosion; tribocorrosion.

## Introdução

O titânio (Ti) possui combinação favorável de propriedades mecânicas, físicas, químicas e biológicas, como baixa densidade, alta resistência mecânica, elevada resistência à corrosão e excelente biocompatibilidade, que podem ser melhoradas com a adição de elementos de liga<sup>34,35,37,56,57</sup>. Como exemplo, a liga Ti6Al4V é muito utilizada para aplicações biomédicas.

Sabe-se que a liga em si é biocompatível<sup>17</sup>, porém, é conhecida a toxicidade dos elementos alumínio (Al) e vanádio (V), na forma de íons ou partículas de desgaste<sup>5,20,38,54,61,62,66,73</sup>. Rao et al.<sup>66</sup> e Okazaki et al.<sup>61</sup> investigaram o crescimento de fibroblastos (L-929) e osteoblastos (MC3T3.E1) quando em contato com partículas metálicas de Ti, Al e V. Observou-se que nos meios controle e contendo Ti, o crescimento dessas células foi similar. Porém, o crescimento das células foi menor nos meios contendo Al e V. Portanto, Al e V podem comprometer a osseointegração.

Além disso, o Al contribui para a patogênese de doenças neurológicas, como o mal de Alzheimer<sup>62</sup>. A toxicidade do Ti e do V é controversa. Há estudos que relacionam o V com o mal de Parkinson<sup>54</sup> e outros com o comprometimento da reprodução, gestação e lactação<sup>20</sup>. Além disso, o Ti pode causar reações alérgicas<sup>73</sup>.

Com o aumento da expectativa de vida da população, aliado ao uso cada vez mais comum de implantes ortopédicos e dentários, torna-se válido o estudo de novos dispositivos que sejam biocompatíveis e que tenham maior durabilidade. Estes não precisam necessariamente ser fabricados a partir de novos materiais, mas sim de materiais modificados para obtenção de melhores propriedades, como por diversificação das



composições químicas, tratamentos térmicos e modificação de superfícies.

O Ti possui duas estruturas cristalinas, conhecidas como fases  $\alpha$  e  $\beta$ . A fase  $\alpha$  está relacionada à estrutura estável em temperatura ambiente, a qual é denominada estrutura hexagonal compacta (hc). Ao elevar a temperatura a aproximadamente 883°C, a fase  $\alpha$  transforma-se em  $\beta$ , representada por uma estrutura cúbica de corpo centrado (ccc)<sup>3,10,21</sup>. Essa temperatura é conhecida como a  $\beta$ -transus do titânio, que corresponde a menor temperatura em que o material é 100%  $\beta$ <sup>4</sup>.

Com a adição de elementos de liga ao Ti, obtêm-se ligas com estruturas cristalinas estáveis em temperatura ambiente. As fases  $\alpha$  e  $\beta$  são base para três tipos de ligas de Ti:  $\alpha$ ,  $\alpha+\beta$  e  $\beta$ , que têm suas estruturas relacionadas com o tipo de elemento de liga utilizado<sup>25</sup>. Os elementos de liga podem ser classificados como  $\alpha$ -estabilizador,  $\beta$ -estabilizador e neutro. O primeiro promove o aumento da temperatura de transformação da fase  $\alpha$  para a fase  $\beta$  quando adicionado ao Ti, o segundo diminui essa temperatura e o terceiro não altera a transformação de fases<sup>3,39</sup>. Como exemplos de  $\alpha$ -estabilizadores têm-se: alumínio (Al), oxigênio (O) e nitrogênio (N) e, de  $\beta$ -estabilizadores têm-se: vanádio (V), tântalo (Ta), nióbio (Nb), molibdênio (Mo), magnésio (Mg) e ferro (Fe)<sup>3,21</sup>. O zircônio (Zr) e o estanho (Sn) são elementos neutros<sup>3</sup>.

As ligas  $\alpha$  são formadas a partir de elementos  $\alpha$ -estabilizadores e, em temperatura ambiente, apresentam apenas a fase  $\alpha$  e, portanto tem estrutura hc. Essas ligas têm características satisfatórias de resistência mecânica, tenacidade e soldabilidade<sup>10</sup>, as quais não podem ser melhoradas a partir de tratamentos térmicos<sup>3</sup>.

As ligas  $\alpha+\beta$  frequentemente contêm elementos  $\alpha$ - e  $\beta$ -estabilizadores, mas podem conter apenas  $\beta$ -estabilizadores. Essas ligas são formuladas para que a fase  $\alpha$  coexista com a fase  $\beta$ , em temperatura

ambiente<sup>10,21</sup>. Essas ligas geralmente apresentam boa conformação e resistência mecânica em temperatura ambiente<sup>10</sup>. As propriedades das ligas  $\alpha+\beta$  podem ser modificadas por meio de tratamentos térmicos<sup>3,25</sup>.

As ligas  $\beta$  são formadas quando elementos  $\beta$ -estabilizadores são adicionados ao Ti e, dependendo da quantidade desses elementos e dos tratamentos térmicos aplicados, obtém-se melhoria nas propriedades mecânicas desse tipo de liga<sup>30</sup>. À temperatura ambiente, essas ligas apresentam predominância da fase  $\beta$ , e a estabilização da estrutura ccc está relacionada com as características de baixo módulo de elasticidade, e elevada resistência mecânica<sup>46</sup>.

Os tratamentos térmicos promovem transformação de fases e mudança na microestrutura das ligas de Ti, que estão relacionadas com o aprimoramento das suas propriedades<sup>25</sup>. As ligas que contêm baixo teor de elementos  $\beta$ -estabilizadores, além de apresentarem as duas fases sólidas estáveis,  $\alpha$  e  $\beta$ , podem levar à formação de fases metaestáveis, correspondentes às fases martensíticas ( $\alpha'$ - fase martensítica do tipo hexagonal compacta e  $\alpha''$ - fase martensítica do tipo hexagonal ortorrômbica) e  $\omega$  (fase metaestável do tipo hexagonal compacta ou trigonal), durante o tratamento térmico<sup>19,58,75</sup>.

De acordo com esses dados, novas ligas de Ti, a partir do sistema TiNbZr, têm sido formuladas, a serem utilizadas nas áreas médica e odontológica. O Zr, além de neutro, é um agente endurecedor de solução sólida e possui propriedades semelhantes às do Ti. O Nb é um elemento estabilizador de fase  $\beta$ , que está relacionado com a melhora das propriedades mecânicas do material. Ao elaborar novas ligas para o uso, como biomaterial na área biomédica, é importante investigar propriedades, como biocompatibilidade, módulo de elasticidade, resistência à corrosão e ao desgaste.

Wang et al.<sup>79</sup> (2010) reportaram alta citocompatibilidade (fibroblastos L-929) da liga Ti22Nb4Zr quando comparada àquela do Ti comercialmente puro (Ti cp) e a um controle negativo. Cremasco et al.<sup>17</sup> (2011) confirmaram esse resultado ao concluírem que o Ti cp e algumas ligas de Ti, dentre elas Ti6Al4V e Ti25Nb15Zr, não apresentaram comportamento citotóxico e possuíram boa adesão de fibroblastos (células Vero, provenientes de macacos verdes africanos, *Cercopithecus aethiops*) em suas superfícies após 24h de cultura celular.

O módulo de elasticidade é um fator importante quando o material é desenvolvido para substituir ou interagir com o osso. Este deve ter um valor semelhante ao do tecido ósseo ao redor do implante para possibilitar a reparação e a remodelação óssea<sup>63,65</sup>. O Ti cp e a liga Ti6Al4V possuem módulo de elasticidade de aproximadamente 105GPa<sup>55</sup>, que é mais elevado que o módulo do tecido ósseo, entre 10 e 30GPa<sup>26,57,58,63</sup>. Estudos mostram que as ligas  $\beta$  possuem módulo de elasticidade mais próximo ao do osso<sup>1,11,58</sup>.

A resistência à corrosão está diretamente relacionada com a biocompatibilidade do material. Sabe-se que, quando o Ti entra em contato com o oxigênio, há a formação de uma camada de óxidos na sua superfície, com aproximadamente  $\leq 10\text{nm}$  de espessura, que confere proteção ao metal<sup>8,21</sup>.

O filme passivo do Ti é composto predominantemente de TiO<sub>2</sub><sup>21</sup>. Já as ligas de Ti podem ter composição variada de óxidos, dependendo dos elementos de liga presentes que podem modificar a propriedade protetora do óxido de Ti. Por exemplo, sabe-se que o Nb leva à formação de Nb<sub>2</sub>O<sub>5</sub>, o Zr, ZrO<sub>2</sub>, o Ta, Ta<sub>2</sub>O<sub>5</sub>, o V, VO<sub>2</sub> e o Al, Al<sub>2</sub>O<sub>3</sub>. E, que o óxido de Ti modificados pelos óxidos de Nb, Zr e Ta apresentam melhor estabilidade e, portanto, podem conferir melhor proteção do que pelos óxidos de Al e V<sup>27,48,49</sup>.

Entretanto, quando em meios agressivos, o filme passivo pode ser deteriorado com a remoção da camada de óxidos, levando à corrosão do metal base. Fato esse que deve ser evitado quando se trata de implantes, pois os produtos de corrosão podem causar alergia local ou ainda, entrar em contato com a corrente sanguínea e serem acumulados em diferentes órgãos, causando injúrias ao organismo humano<sup>77</sup>.

Essa propriedade pode ser avaliada pelo comportamento eletroquímico do material, ou seja, pelo potencial de circuito aberto, espectroscopia de impedância eletroquímica e polarização potenciodinâmica. De uma maneira geral, com esses métodos é possível analisar, respectivamente, variação de potencial com o tempo, resistência à polarização e capacitância, velocidade de corrosão e tendência à corrosão.

A maioria das novas ligas em desenvolvimento está relacionada com próteses ortopédicas e, normalmente, as soluções utilizadas nos testes de resistência à corrosão são Ringer, Hank, NaCl e, também, soluções contendo proteínas<sup>6,7,15,32,70</sup>.

Assis et al.<sup>7</sup> (2008) investigaram a resistência à corrosão da liga Ti13Nb13Zr em NaCl a 0,9%, solução de Hank e em meio essencial mínimo que contém sais inorgânicos, aminoácidos e vitaminas. Observou-se que a liga possui comportamento passivo nos três eletrólitos estudados.

Ao comparar o comportamento eletroquímico entre as ligas Ti13Nb13Zr e Ti6Al4V, Robin et al.<sup>70</sup> (2008) observaram que a liga Ti13Nb13Zr obteve maior resistência a corrosão em solução de Ringer. Choubey et al.<sup>15</sup> (2005) demonstraram que a liga Ti13Nb13Zr teve uma taxa de corrosão ligeiramente menor comparada à liga Ti6Al4V em solução de Hank. O mesmo foi observado por Assis, Costa<sup>6</sup> (2007) quando as ligas ficaram imersas em solução de Hank durante 410 dias.

Sabe-se que as ligas de Ti sempre apresentam corrosão, e, na cavidade bucal, não só a microestrutura do biomaterial<sup>44</sup> é fator modificador do seu comportamento eletroquímico, como também a temperatura, quantidade e qualidade da saliva<sup>82</sup> placa bacteriana<sup>12</sup>, pH<sup>40,67,74,78</sup> proteínas<sup>32</sup>, propriedades físicas e químicas dos alimentos e bebidas, além de produtos de higiene oral<sup>13</sup>.

Quando ocorre corrosão, as superfícies dos conjuntos implantes-componentes protéticos podem ficar mais rugosas, facilitando a instalação de micro-organismos. A partir da instalação e acúmulo de micro-organismos, uma reação inflamatória pode ser iniciada e, devido à resposta do hospedeiro, pode ocorrer o desenvolvimento de peri-implantite, a qual, se não tratada, poderá causar destruição óssea ao redor do implante com consequente perda do mesmo<sup>53,59,69,72</sup>. Estudos mostram que a rugosidade das superfícies de biomateriais, utilizados na confecção de implantes, causada por corrosão, em diferentes meios agressivos, pode favorecer o acúmulo de micro-organismos<sup>9,16,53,69,72</sup>.

Além disso, é importante salientar que as superfícies citadas também podem apresentar desgaste mecânico. Portanto, o estudo da tribocorrosão do Ti e de suas ligas é interessante, uma vez que unifica as propriedades mecânicas e químicas. Ou seja, a tribocorrosão é o efeito sinérgico causado pela ação combinada da corrosão com o mecanismo de desgaste mecânico<sup>24,36,64,78</sup>.

Há diversos sistemas de tribocorrosão como *pin-on-disc* e *ball-on-plate*<sup>50</sup>, em que um material é deslizado sobre o outro, imersos em banho de eletrólito, causando desgaste e também remoção do filme passivo. Assim, o material base fica exposto à solução e mais sujeito à corrosão. Tanto o desgaste como o eletrólito influenciam no processo de corrosão, já que estão agindo concomitantemente. Entretanto, é válido explicar que, durante o procedimento, o material pode apresentar tanto a

depassivação como a repassivação, já que é um sistema de deslizamento<sup>36</sup>.

Há a possibilidade de estudar a relação entre dois materiais ou o comportamento de um material utilizando um antagonista quimicamente inerte. Além disso, a amplitude do deslizamento pode ser modificada, assim como o eletrólito. A partir dos resultados obtidos, é possível caracterizar o material quanto à deformação, ao volume de desgaste e à capacidade de repassivação do filme protetor.

Conseqüentemente, o estudo do processo de tribocorrosão dos materiais utilizados para a fabricação de conjuntos implantes-componentes protéticos é de fundamental importância. O Ti e suas ligas, além de estarem sujeitos a ambiente químico agressivo, possuem, geralmente, baixa resistência ao desgaste<sup>29,41</sup>.

Assim como nos estudos de corrosão, a maioria dos trabalhos sobre tribocorrosão de ligas de Ti tem enfoque nos implantes ortopédicos. Majumdar et al.<sup>43</sup> (2008) avaliaram o desgaste mecânico da liga Ti13Nb13Zr com carga aplicada de 50N, com diferentes microestruturas ( $\alpha$ ,  $\beta$  e martensítica), a seco, em solução de Hank e em soro bovino. De uma maneira geral, a microestrutura não influenciou a taxa de desgaste a seco. E, independentemente da microestrutura, o dano à liga aumentou quando testadas em soluções fisiológicas, apresentando essencialmente desgaste por abrasão.

More et al.<sup>52</sup> (2011) verificaram o comportamento tribocorrosivo (com carga aplicada de 6,5N) da liga Ti13Nb13Zr em solução de Hank. Constatou-se que a liga teve tendência a repassar durante o deslizamento e ao final do ensaio, quando o potencial foi restabelecido. Portanto, o comportamento eletroquímico e as propriedades da superfície da liga não foram afetados significativamente.

Ao comparar as ligas Ti13Nb13Zr e Ti6Al4V, Choubey et al.<sup>14</sup> (2004) observaram grave desgaste em ambas as ligas após ensaio de tribocorrosão com carga aplicada de 10N em solução de Hank. Cvijović-Alagić et al.<sup>18</sup> (2011) investigaram o comportamento mecânico e eletroquímico isoladamente, concluindo que a liga martensítica Ti13Nb13Zr apresentou menor resistência ao desgaste mecânico, com carga aplicada de 40N, porém, maior resistência à corrosão, em solução de Ringer, comparada à liga  $\alpha+\beta$  Ti6Al4V. Entretanto, não há na literatura relatos sobre o comportamento tribocorrosivo das ligas TiNbZr em saliva artificial com baixas cargas.

Apesar da estabilidade da camada superficial de óxidos e das boas propriedades mecânicas das ligas de Ti, o sucesso em longo prazo de implantes e estruturas protéticas depende da interação do metal com o ambiente oral<sup>23</sup> devido às reações químicas e eletroquímicas<sup>51</sup>, às forças mecânicas resultantes da mastigação, à interação entre os componentes dos sistemas implante/osso e implante/prótese e ao desgaste<sup>31</sup>.

Novas ligas de Ti com Nb e Zr adicionados têm sido investigadas para aplicação como biomaterial, porém ainda não existe um consenso quanto à porcentagem em massa desses metais bem como o processo de fabricação. Ao pesquisar novos materiais, sugere-se seguir etapas. A primeira etapa consiste em estudar as propriedades fundamentais físicas, químicas e mecânicas do material. A segunda etapa é dirigida ao estudo das propriedades relacionadas com a sua aplicação, como a resistência à corrosão e ao desgaste quando no desenvolvimento de materiais para confecção de conjuntos implantes-componentes protéticos. Seguindo esse objetivo, na terceira etapa, realizam-se testes biológicos, primeiramente in vitro e depois in vivo para avaliar, principalmente, processos de inflamação e capacidade de osseointegração.

A partir dos conceitos citados, tivemos a premissa de desenvolver duas novas ligas Ti35Nb5Zr e Ti35Nb10Zr para serem utilizadas na confecção de implantes e componentes protéticos dentários. Na elaboração das ligas de Ti, quanto às proporções dos elementos Nb e Zr, considerou-se a importância do baixo módulo de elasticidade para biomateriais utilizados como implantes cirúrgicos<sup>26,28,33,63,65,80,83</sup>. E, como citado anteriormente<sup>58</sup>, as ligas de Ti tipo  $\beta$  possuem tal propriedade. O Nb mostrou-se eficiente como  $\beta$  estabilizador a 35%<sup>1</sup>. Porém, o Nb também promove a precipitação de fase  $\omega$ , a qual aumenta o módulo de elasticidade<sup>1,30</sup>. O Zr, além da função de solidificador de fase sólida, também inibe a formação da fase  $\omega$ . Conseqüentemente, o Zr foi utilizado em duas concentrações, 5 e 10%, para verificar a sua atuação nas ligas.

Em um primeiro momento, as ligas foram fundidas e caracterizadas quanto às suas propriedades mecânicas, físicas e químicas<sup>68</sup>. Os resultados mostraram composição química final muito semelhante à nominal. A liga Ti35Nb5Zr apresentou fases  $\alpha$  e  $\beta$  em sua estrutura, e a liga Ti35Nb10Zr, apenas fase  $\beta$ . Apesar da diferença microestrutural, os resultados dos testes de dureza, tração e ciclagem mecânica sugeriram que as duas ligas eram promissoras para alcançar o objetivo proposto.

Seguindo a proposta de etapas do estudo de um novo material, o objetivo dessa tese foi avaliar a resistência à corrosão das novas ligas Ti35Nb5Zr e Ti35Nb10Zr, utilizando as análises: potencial de circuito aberto com o tempo, espectroscopia de impedância eletroquímica e polarização potenciodinâmica, variando o tempo de 0,5h a 216h. E, também, avaliar a tribocorrosão das novas ligas aplicando diferentes cargas, 50mN a 1N. Nos diferentes testes, utilizou-se solução de saliva artificial, a 37°C, como eletrólito. A liga comercial Ti6Al4V foi estudada nas mesmas condições, com a finalidade de comparação.



Para complementar a interpretação dos resultados realizou-se o teste de dureza Vickers e a espectroscopia de raios-X.

O desenvolvimento da tese resultou dois trabalhos, relatados na forma de capítulos:

Capítulo 1: Are new TiNbZr alloys potential substitutes for the Ti6Al4V alloy for dental applications? A corrosion view

Capítulo 2: On the tribocorrosion of new Ti35Nb5Zr and Ti35Nb10Zr alloys for dental applications: passive film vs. bulk behaviour

## **Capítulo 1**

**Are new TiNbZr alloys potential substitutes for the Ti6Al4V alloy for dental applications? A corrosion behaviour view**

Manuscrito submetido para publicação – Biomaterials, março 2012.

Are new TiNbZr alloys potential substitutes for the Ti6Al4V alloy for dental applications? A corrosion behaviour view

Ana Lúcia Roselino Ribeiro<sup>1\*</sup>, Luís Geraldo Vaz<sup>2</sup>

<sup>1</sup>Departamento de Diagnóstico e Cirurgia, Faculdade de Odontologia de Araraquara, UNESP Univ Estadual Paulista, Araraquara, Brazil

<sup>2</sup>Departamento de Materiais Odontológicos e Prótese, Faculdade de Odontologia de Araraquara, UNESP Univ Estadual Paulista, Araraquara, Brazil

\*Corresponding author:

Address: Rua Humaitá, 1680. FOAr-UNESP. 14801-903. Araraquara-SP, Brazil.

Phone number: +55 16 33016420

e-mail: analuciaroselino@yahoo.com.br

**Title**

Are new TiNbZr alloys potential substitutes for the Ti6Al4V alloy for dental applications? A corrosion behaviour view

**Abstract**

The success of metallic dental implants is, in part, related to its mechanical resistance, corrosion behaviour and biocompatibility. The corrosion resistance of implant is strongly dependent on the properties of the oxide film formed on its metal surface. Metallic particles and ions resulting from the corrosion process can be harmful to the living organism and ultimately lead to implant failure. Objectives: The objective of this work was to assess the electrochemical behaviour of new Ti35Nb5Zr and Ti35Nb10Zr alloys in artificial saliva at 37°C to establish if they are indicated to be used as biomaterials in dentistry as alternative to Ti6Al4V alloys, considering the corrosion properties of the material. Methods: electrochemical impedance spectroscopy (EIS) experiments were carried for different periods of time (0-216h) in a three electrode cell, where the working electrode (Ti alloy) was exposed to artificial saliva at 37°C. A saturated calomel electrode and a platinum electrode were used as reference and counter electrode, respectively. Results: all alloys exhibited an increase of the corrosion potential with the immersion time, indicating the growth and stabilization of the passive film. Ti35Nb5Zr and Ti6Al4V alloys had their EIS results interpreted by a double-layer circuit while the Ti35Nb10Zr alloy was modeled by one-layer circuit. In general, Ti35Nb10Zr alloy had better electrochemical behaviour when compared with the Ti6Al4V alloy probably due to their oxide film structure and composition ( $\text{TiO}_2$ ,  $\text{Nb}_2\text{O}_5$ ,  $\text{ZrO}_2$ ). Significance:

Nb and Zr enhanced corrosion resistance, which is interesting because indicates that the new Ti35Nb10Zr alloy may be used in the dental implants manufacturing.

**Key words:** dental implants; titanium alloys; corrosion; artificial saliva.

## 1. Introduction

Dental caries and periodontal diseases may lead to tooth loss, which can cause disorder in the quality of life, because it affects the health and appearance of the individuals [1]. Therefore, dental implants can be used to replace missing teeth. With the increasing in longevity of general population, implants should keep long-life functionality.

Implants success relies on a large variety of parameters such as clinical procedure (treatment planning and installation procedure), biomaterial characteristics (mechanical properties, biocompatibility and electrochemical performance), manufacturing process, implant design and physiologic solutions [2,3]. If inadequate, implants can lead to lack of osseointegration.

Osseointegration is the close apposition of the bone to the implant surface and is strongly dependent to the properties of the oxide film (passive film), which is naturally formed on the surface of metallic biomaterials [4]. In fact, the implant oxide film is in directly contact to the bone. In addition, the oxide film is also associated with the materials biocompatibility as it is responsible for its resistance to corrosion [5]. If the passive film is removed, the bulk metal of the implant may become unprotected. This can lead to the metal corrosion and then increasing the possibility of its degradation.

Metallic biomaterials in contact with physiological solution undergo corrosion. Most of the studies on this topic is related to orthopedic implants but it seems that the dental implants undergo the same complexities. In general, the metallic particles resulting from the implant degradation process can cause local infection [6,7,8], affect cell metabolism [9,10,11] and be accumulated in organs

[12] leading to systemic diseases [13,14]. Therefore, they can be harmful to the living organism and can also lead to implant failure by lack of osseointegration [7,8]. Hence, it is important to verify the oxide layer formed on the implant surface as achieve its improvement.

The material of choice for dental implant-abutment sets fabrication is titanium (Ti) and its alloys. The most common used alloy is Ti6Al4V. Even though some studies show that this is a biocompatible alloy [15], the toxicity of vanadium (V) and aluminum (Al) started to appear in the last years. Rao et al. [16] and Okazaki et al. [17] investigated cell growth of fibroblasts (L-929) and osteoblasts (MC3T3.E1) front of metallic powders of Ti, Al and V. They verified that on control and Ti containing media, the fibroblasts and osteoblasts growth rate were almost similar. However, the cells growth rate decreased when in contact to Al and V. Therefore, Al and V may compromise osseointegration. In addition, as it is found the presence of particulate debris on the tissues around failure implants as in distant organs, it is important to be aware of the potential toxicity of each alloying element. The contribution of Al on the pathogenic process of neurological diseases as Alzheimer, when it is accumulated in brain, is established [13]. However, V and Ti toxicity is unclear. There are studied that relates V to Parkinsonian dementia [14] or to injuries on reproduction, gestation and lactation [18], and Ti to allergenic reaction [19].

Considering that Ti and Ti alloys have good mechanical and corrosion resistance [5], in last years, efforts are being made towards the development of new high resistant and biocompatible titanium alloys, such as TiNbZr [20,21]. In fact, niobium (Nb) is a  $\beta$ -stabilizer resulting on the improvement of the

mechanical characteristics of the alloy, together with the solid solution hardening effect of zirconium (Zr). TiNbZr alloys are known to be no toxic [15,22,23,24]. In fact, Wang et al. [23] reported a high cytocompatibility (L-929 fibroblasts) and hemocompatibility for the Ti<sub>22</sub>Nb<sub>4</sub>Zr alloy, indicating that the addition of Nb and Zr to Ti do not lead to cytotoxicity in comparison to a negative control and commercially pure Ti (CP Ti). Additionally, Cremasco et al. [15] investigated the cytotoxicity and fibroblast cell adhesion on CP Ti and some Ti alloys, among them, Ti6Al4V and Ti<sub>25</sub>Nb<sub>15</sub>Zr. It was concluded that these cited alloys had in vitro cytocompatibility since they did not have toxic behaviour and had good cell adhesion, after 24h of cell cultivation. However, none is known about the toxicology of Nb and Zr ions and corrosion particles to human body.

Most of the studies on electrochemical behaviour of Ti6Al4V is related to its application as orthopedic implants. Therefore, the corrosion resistance of this alloy is mainly documented in Hank's [25-28] and Ringer's [29] solutions (composed by inorganic ions equivalent to the ones found in the body) and in solutions with proteins addition [30,31]. Fewer studies were accomplished in artificial saliva [32-34]. In general, it was observed, independently of the solution, a remarkable corrosion resistance as a passive metal behaviour. Essentially, the protective oxide film formed on Ti6Al4V is composed of TiO<sub>2</sub> [6]. Besides, the cited studies, realized with artificial saliva, investigated the solution change by pH variation [33] and addition of fluoride ions on acidic saliva [32,34]. Barao et al. [33] verified that in acidic saliva, less protective oxide film was formed on Ti6Al4V surface. Schiff et al. [32] and Huang [34] observed a



negatively influence of fluoridated–acidified solution on the alloy corrosion resistance due to damage of the passive film.

Ti13Nb13Zr was investigated by Assis et al [35] by means of corrosion resistance in 0.9% NaCl solution, Hank's solution and minimum essential medium (composed by inorganic salts, amino acids and vitamins). The alloy showed passive behaviour in all three electrolytes.

When comparing the electrochemical behaviour of both cited alloys, Robin et al. [36] observed that Ti13Nb13Zr presented higher resistance to corrosion in Ringer's solution. Choubey et al. [25] demonstrated that Ti13Nb13Zr had lower corrosion rates than Ti6Al4V in Hank's solution. The same observation was found by Assis and Costa [27] when the alloys were immersed in Hank's solution for 410 days.

In a previous study [21], Ti35Nb5Zr and Ti35Nb10Zr alloys showed good mechanical resistance. As it is intended to use these alloys for the development of dental implant-abutment sets, it is important to study their corrosion behaviour in artificial saliva.

Therefore, the objective of this investigation was to assess the electrochemical behaviour of new Ti35Nb5Zr and Ti35Nb10Zr at different periods of time, in artificial saliva at 37°C. The results were compared to the ones of commercial Ti6Al4V alloy. The null hypothesis of the study was that the new TiNbZr alloys could be substitutes for the Ti6Al4V for dental applications.

## 2. Materials and methods

The electrochemical behaviour of new  $\alpha+\beta$  Ti35Nb5Zr and  $\beta$  Ti35Nb10Zr alloys [21] were studied at different periods of time (from 0h to 216h) in an artificial saliva solution, similar to that described by Fusayama et al. [37] (Table 1), 5.25 pH at 37°C. This temperature had been chosen because is the human body one. It is important to control it because the material electrochemical behaviour can be changed by temperature due to the growth of passive film on its surface [28].  $\alpha+\beta$  Ti6Al4V alloy was also studied for comparison purpose.

Table 1 - Chemical composition of artificial saliva (g/l)

NaCl	KCl	CaCl <sub>2</sub> .2H <sub>2</sub> O	Na <sub>2</sub> S.9H <sub>2</sub> O	NaH <sub>2</sub> PO <sub>4</sub> .2H <sub>2</sub> O	Urea
0.4	0.4	0.795	0.005	0.69	1

The TiNbZr alloys were arc melted from pure metals, using a water-cooled copper hearth under an argon atmosphere. The ingots were flipped and remelted 3-5 times to ensure chemical homogeneity. After that, the obtained ingots were heat treated at 1000°C for 8h and furnace cooled. Then, they were hot-forged in 10mm diameter bars and machined as discs (8mm diameter x 8mm height). Thereafter, the samples were heat treated at 1000°C for 1h and air cooled in order to relieve stress generated during the machining. The Ti6Al4V alloy was machined as discs (25mm diameter x 4.5mm height) from acquired bar stock.

Afterward, all three alloys samples were mechanically polished with emery papers until #1200, ultrasonically cleaned with acetone, etched with Kroll's reagent (1ml HF, 5ml HNO<sub>3</sub>, 44ml distilled water), ultrasonically cleaned with propanol and after with distilled water followed by hot drying.

### **2.1. Surface analysis**

The X-ray spectroscopy (XPS) analysis was carried out at a pressure of less than 10<sup>-6</sup>Pa using a commercial spectrometer (UNI-SPECS UHV) to verify the changes in surface chemical composition of the alloys studied. The Mg K $\alpha$  line was used ( $h\lambda = 1253.6\text{eV}$ ) and the analyzer pass energy was set to 10eV. The inelastic background of the Nb 3d, Zr 3d, V 2p, Al 2p, Ti 2p, O 1s, C 1s, Ca 2p and P 2p electron core-level spectra was subtracted using Shirley's method. The composition of the near surface region was determined with an accuracy of  $\pm 10\%$  from the ratio of the relative peak areas corrected by Scofield's sensitivity factors of the corresponding elements. The spectra were fitted without placing constraints using multiple Voigt profiles. The width at half maximum (FWHM) varied between 1.1 and 2.1eV and the accuracy of the peak positions was  $\pm 0.1\text{eV}$ .

The analyses were accomplished 24h after the samples attack with Kroll's reagent and after 216h of samples immersion in artificial saliva at 37°C. The samples were ultrasonically cleaned with propanol, hot water (60°C) and hot drying.

## 2.2. Electrochemical analysis

After 24h of the samples cleaning, the electrochemical impedance spectroscopy (EIS) experiments were carried out at open circuit potential ( $E_{\text{corr}}$ ) with frequencies ranging from 63kHz to 10mHz and Ac voltage of 10mV/ms, in different periods of time (0.5-216h). The EIS results were assessed using Gamry framework software. And the quality of fitting was evaluated by the Goodness of fitting values ( $<10^{-3}$ ). The results were statistically analyzed by variance analysis (ANOVA) and then Tukey's test when comparing three alloys and Tukey's test when comparing two alloys ( $\alpha=0.05$ ). The  $E_{\text{corr}}$  values in function of time achieved during EIS analysis were also recorded to verify the passive film behaviour.

After the last measurement at 216h, it was obtained the potentiodynamic polarization curves with a potential range from -0.9 to 2V with respect to E vs. SCE at a scan rate of 1mV/s. The results were statistically analyzed by Kruskal-Wallis test and then Dunn's Multiple Comparison Test ( $\alpha=0.05$ ).

The tests were performed in a three electrode cell, with an O'ring of 0.636cm<sup>2</sup> area where the work electrode (Ti alloys) was exposed. A saturated calomel electrode (SCE) and a platinum electrode were used as reference and counter electrodes, respectively. Therefore, all the potential values are referred to the SCE (Potentiostat: Reference 600, Gamry Instruments, Warminster, PA, USA). Several tests were made and at least three similar results were required to ensure reproducibility.

### 3. Results and discussion

#### 3.1. Surface analysis

The XPS characterization showed the presence of  $\text{TiO}_2$ ,  $\text{Al}_2\text{O}_3$  and  $\text{VO}_2$  on the oxide film formed on Ti6Al4V and  $\text{TiO}_2$ ,  $\text{Nb}_2\text{O}_5$  and  $\text{ZrO}_2$  on the oxide film formed on TiNbZr alloys as the major oxides, independently of the Ti alloys immersion in the artificial saliva as seen in Table 2. The same oxides was found on Ti alloys by Okazaki et al. [38,39] and Yu, Scully [40]. Moreover, CaO and  $\text{PO}_4$  were present on the passive film of Ti alloys that were immersed in artificial saliva.

Table 2 - Percentage of oxides on Ti6Al4V, Ti35Nb5Zr and Ti35Nb10Zr passive films, calculated from XPS results, without alloys immersion and after 216h of alloys immersion in artificial saliva at 37°C.

	without immersion			after 216h of immersion		
	Ti6Al4V	Ti35Nb5Zr	Ti35Nb10Zr	Ti6Al4V	Ti35Nb5Zr	Ti35Nb10Zr
$\text{TiO}_2$	86.53%	59.38%	39.80%	55.47%	43.12%	35.52%
$\text{Al}_2\text{O}_3$	11.60%	-	-	10.17%	-	-
$\text{VO}_2$	1.87%	-	-	1.65%	-	-
$\text{Nb}_2\text{O}_5$	-	36.64%	52.07%	-	24.23%	30.50%
$\text{ZrO}_2$	-	3.98%	8.13%	-	2.43%	3.75%
CaO	-	-	-	13.28%	10.37%	11.50%
$\text{PO}_4$	-	-	-	19.44%	19.85%	18.73%

### 3.2. General Corrosion Behaviour

Figure 1 shows representative potentiodynamic polarization curves obtained for the three alloys. It is possible to observe quite similar curves shapes and that all three alloys can be characterized as passive metals, as seen on the curves behaviour. The average values of the corrosion potential ( $E_{(i=0)}$ ) and the passive current density ( $i_{\text{pass}}$ ) are shown on the figure label and no statistical difference was found among the three alloys ( $p > 0.05$ ). It is worthy to say that  $E$  represents the tendency to corrosion and  $i$ , the corrosion velocity.

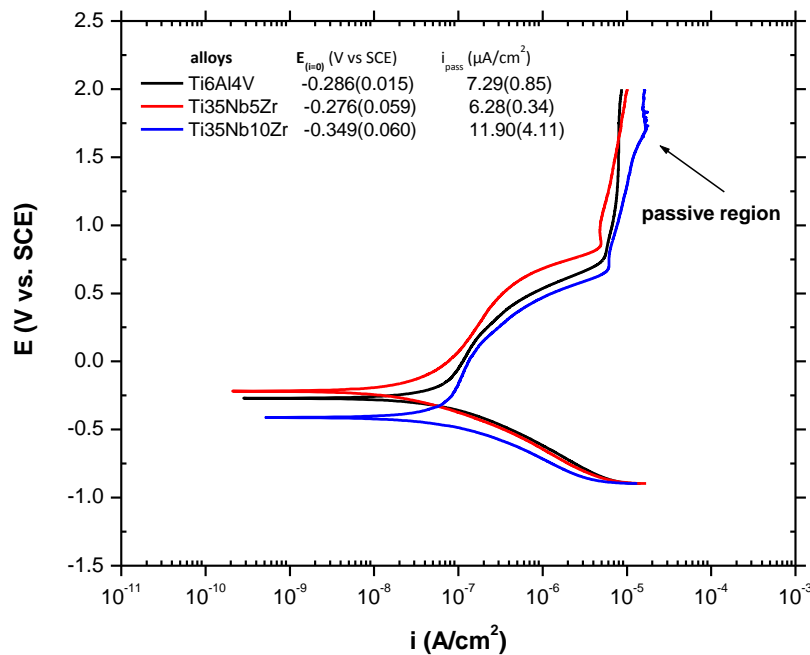


Figure 1 – Potentiodynamic polarization curves obtained for Ti6Al4V, Ti35Nb5Zr and Ti35Nb10Zr in artificial saliva at 37°C, after 216h of open circuit potential. Potential ranged from -0.9 to 2V with scan rate of 1mV/s. The label shows the averages of  $i_{\text{pass}}$  and  $E_{(i=0)}$ . No statistical difference was found among the three alloys considering  $E_{(i=0)}$  and  $i_{\text{pass}}$  results ( $p > 0.05$ ).

Despite of the difficult to compare the results with published data since potential values can be associated to samples preparation, experimental

procedures as oxide film rate formation [27], this result is in accordance to Assis and Costa [27] findings. They observed no difference between Ti6Al4V and Ti13Nb13Zr alloys by means of polarized curves after 410h of alloys immersion in Hank's solution. However, Choubey et al. [25] and Robin et al. [36], when comparing these two alloys, observed a slightly better behaviour of Ti13Nb13Zr in Hank's and Ringer's solution, respectively.

Moreover, Gordin et al. [41] described that  $\beta$ -type Ti12Mo5Ta had the same behaviour of Ti6Al4V after linear and cyclic potentiodynamic polarization curves (Ringer's solution), concluding that the alloys behaviour was not influenced by the chemical composition.

### **3.3. Effect of immersion time on the corrosion behaviour**

#### **3.3.1. Open circuit potential**

The evolution of the open-circuit potential ( $E_{corr}$ ) as a function of time is shown in Figure 2. It represents the potential variation after the alloys had been immersed in artificial saliva. Seeing that the alloys were attacked with Kroll's reagent to remove their oxide films at the same time, 24h before the experiment, the three alloys passive films had the same period of time to grown and then, the measured potentials allow to verify the behaviour of the passive films when the alloys were submerged on the solution as their behaviour in function of immersion time.

As it can be observed in Fig. 2, the  $E_{corr}$  of the three alloys increased during the first 24h and then maintained stable. This is due to the time that is necessary for the transformation of an air-formed oxide film on a metal surface

into an electrical layer when the metal is exposed to an electrolyte, in this study, artificial saliva at 37°C [42].

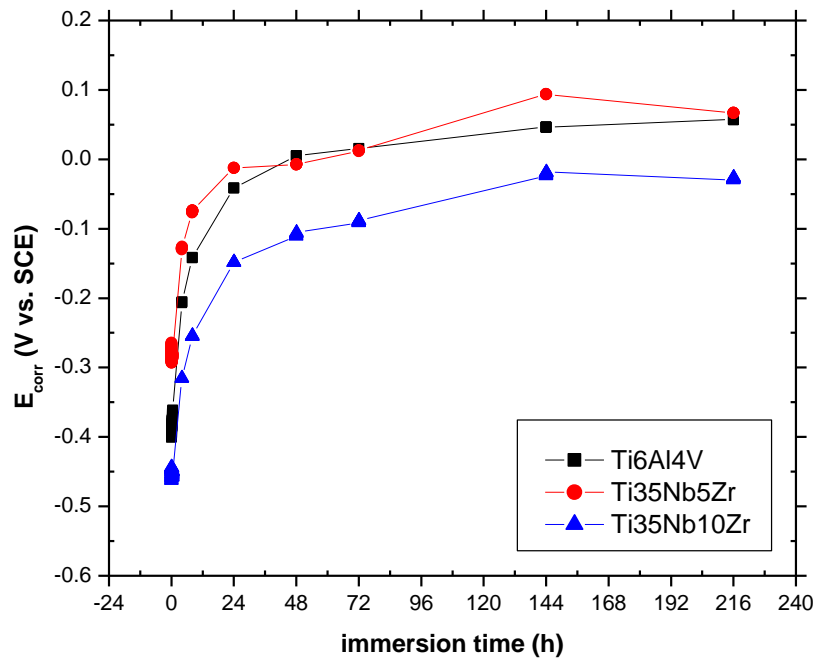


Figure 2 – Open circuit potential behaviour as a function of time of Ti6Al4V, Ti35Nb5Zr and Ti35Nb10Zr alloys in artificial saliva at 37°C.

The behaviour of an  $E_{\text{corr}}$  increasing is positive because it indicates a tendency to form a passive film on the metal surface, when submerged on the electrolyte, which can protect the metal against corrosion [43].

### 3.3.2. Electrochemical impedance spectroscopy

The EIS tests were performed at  $E_{\text{corr}}$  and measured for different times, as referred above, in order to understand the evolution of the corrosion process of the material. The EIS results are presented through Bode diagram (Fig. 3).



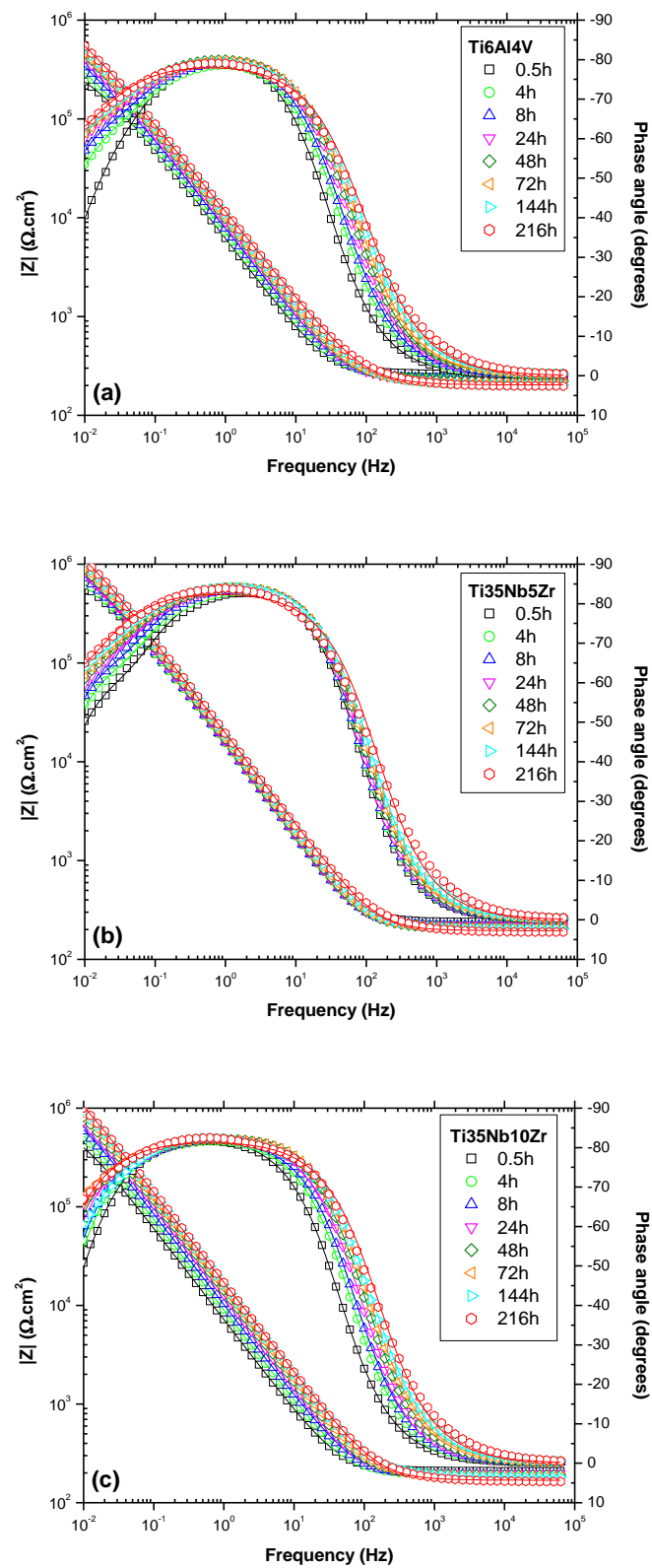


Figure 3 - Bode diagrams of (a) Ti6Al4V, (b) Ti35Nb5Zr, (c) Ti35Nb10Zr – the fitted results (line) were similar to the obtained ones (scatter).

Regardless of the alloy type, it is possible to note in the Bode diagrams the high values of  $|Z|$  and the tendency of the phase angles values to be close to  $90^\circ\text{C}$  in the course of time. These are characteristics of a highly capacitive behaviour suggesting that all three alloys are passive materials and that stable films are formed on them when in contact with the electrolyte [26,44].

Despite these similarities, the alloys EIS spectra were interpreted using different circuits, illustrated in Fig. 4. The experimental data of Ti6Al4V and Ti35Nb5Zr had been modelled using an equivalent circuit that consists of a compact layer and a porous layer (Fig. 4a). The Ti35Nb10Zr data had been interpreted using an equivalent circuit that consists of just one layer (Fig. 4b).

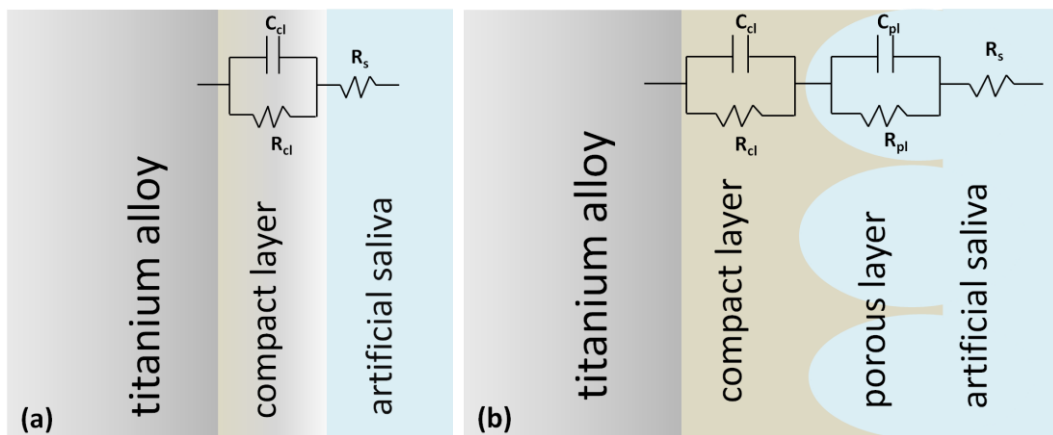


Figure 4 – Equivalent circuits used for the EIS experimental data interpretation: (a) one-layer circuit and (b) two-layer circuit.

The components of both circuits are:

$R_s$  - resistance of the solution

$R_{cl}$  - resistance of the compact layer

$R_{pl}$  - resistance of the porous layer

$C_{cl}$  - capacitance of the compact layer

$C_{pl}$  - capacitance of the porous layer

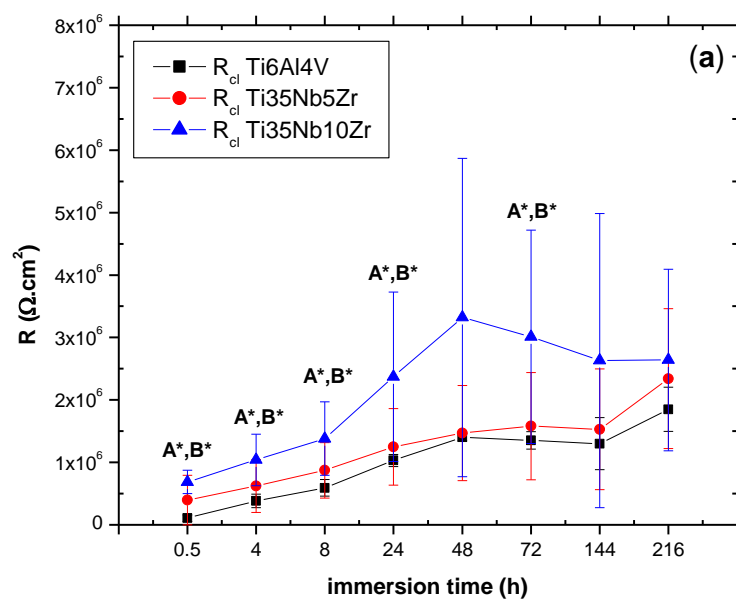
In simple terms,  $R_s$  represents the electrical resistance of the artificial saliva.  $R_{cl}$  and  $R_{pl}$  correspond to the ability of the compact layer and the porous layer of the alloys, respectively, to resist corrosion. In other words, it is the resistance of each layer to transfer ions to the electrolyte. Capacitance represents the amount of charge accumulated on the metal-electrolyte interface. However, constant phase elements ( $CPE_{cl}$ ,  $CPE_{pl}$ ) were used as an alternative to an ideal capacitance element due to electrodes heterogeneities.

According to literature, similar equivalent circuits had been reported before, showing controversy. A similar two-layer circuit had been employed to interpret EIS spectra of Ti-10Mo, Ti-10Mo-10Al, Ti-7Al-4.5V and Ti-5Al-2.5Fe in Ringer's solution [45], Ti6Al4V in Ringer's solution [46], Ti6Al7Nb in Hank's solution [47], Ti6Al4V, Ti6Al7Nb and Ti13Nb13Zr in Hank's solution [26], NiTi in Hank's solution [30].

Barao et al. (2011) [33] interpreted the EIS results of CP Ti and Ti6Al4V in artificial saliva in function of different pH using a circuit similar to the one-layer. The same one-layer was used to fit Ti-Mo EIS results in Ringer's solution [48] and Ti-Ta in artificial saliva [49]. On the other hand, Ibris et al. [50] had shown that CP Ti EIS spectrum suggested the presence of a duplex oxide film while the Ti7Al4.5V and Ti5Al2.5Fe spectrum indicated the existence of one layer oxide film, both in Hank's solution and artificial saliva.

The corrosion resistance of metals can be different depending on the solution used [35]. However, there is evidence that the electrochemical behaviour of titanium alloys is similar in artificial saliva without fluoride ions and Hank's solution [50].

Figure 5 shows the corrosion resistances values in function of time for the three alloys. On Fig. 5a it is possible to verify that the  $R_{cl}$  values of Ti35Nb10Zr remained statistical superior to the other alloys ( $p < 0.05$ ) during the whole experiment, except at the periods of 48h, 144h and 216h that no statistical difference was found. It reached the maximum value at 48h and 72h, in the order of  $3.0 \times 10^6 \Omega \cdot \text{cm}^2$  and then had the tendency to stabilize at the final periods, in the order of  $2.5 \times 10^6 \Omega \cdot \text{cm}^2$ . The other two alloys that were modelled with a one-layer circuit had their values of  $R_{cl}$  similar ( $p > 0.05$ ) and with the tendency of passive film enhancement, reaching values around  $2.0 \times 10^6 \Omega \cdot \text{cm}^2$ . It indicates the reducing of the ion rate release and the growth of oxide layer [35].



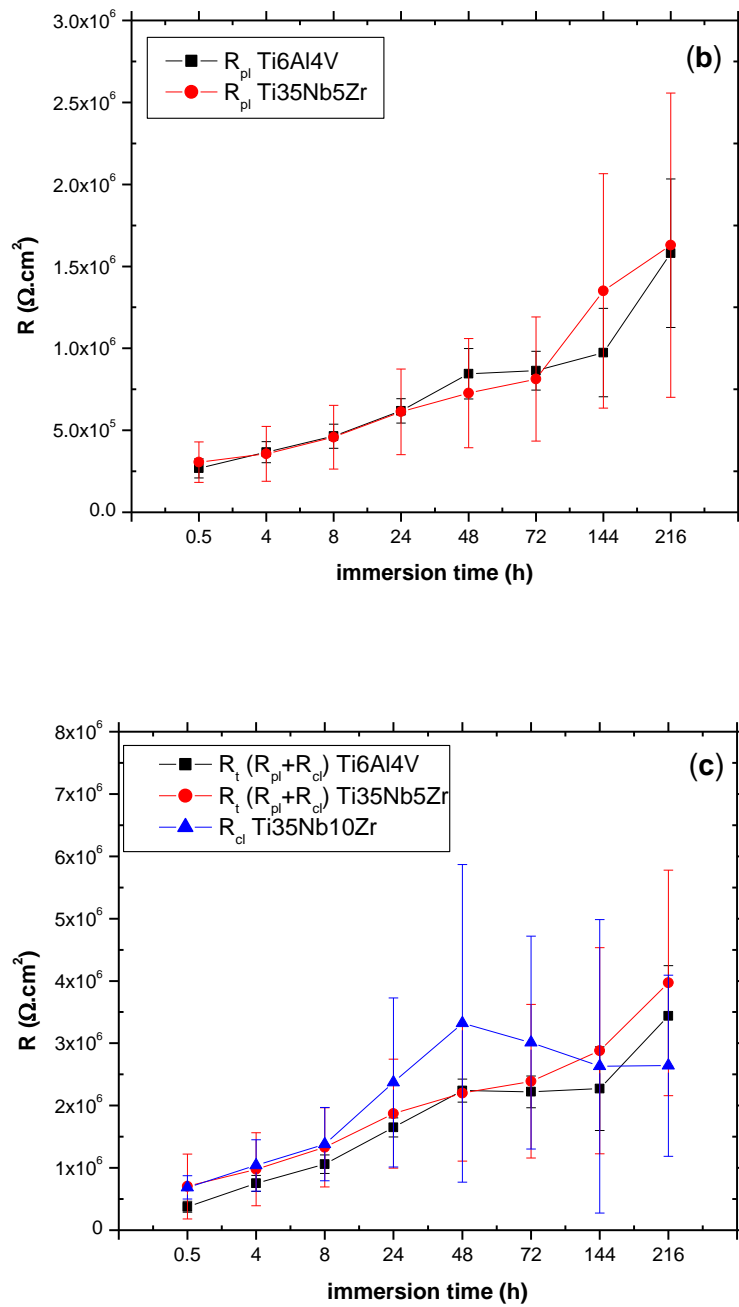


Figure 5 –Averages and standard deviations of (a)  $R_{cl}$ , (b)  $R_{pl}$  and (c)  $R_t$  ( $R_{pl} + R_{cl}$ ) and  $R_{cl}$  in function of time for Ti6Al4V, Ti35Nb5Zr and Ti35Nb10Zr. Statistical difference between Ti alloys in each period of time was calculated by ANOVA and Tukey's test (\* $p < 0.05$ ). (a) - letter **A** shows statistical difference of Ti35Nb5Zr vs. Ti35Nb10Zr and letter **B** shows statistical difference of Ti6Al4V vs. Ti35Nb10Zr, no statistical difference was found between Ti6Al4V vs. Ti35Nb5Zr ( $p > 0.05$ ). (b) and (c) - no statistical difference was found among the three alloys.

The  $R_{pl}$  values (Fig. 5b) were also alike for Ti6Al4V and Ti35Nb5Zr ( $p>0.05$ ) and with the tendency of increase on the last periods. This behaviour can be related to the oxides CaO and  $PO_4$  found on passive film, by XPS analysis (Table 2), after Ti alloys immersion in artificial saliva, in accordance to Assis et al. [35]. They suggested that there are microscopic porous on the porous layer formed on Ti alloys surface, which may incorporate electrolyte components and may lead to resistance increase.

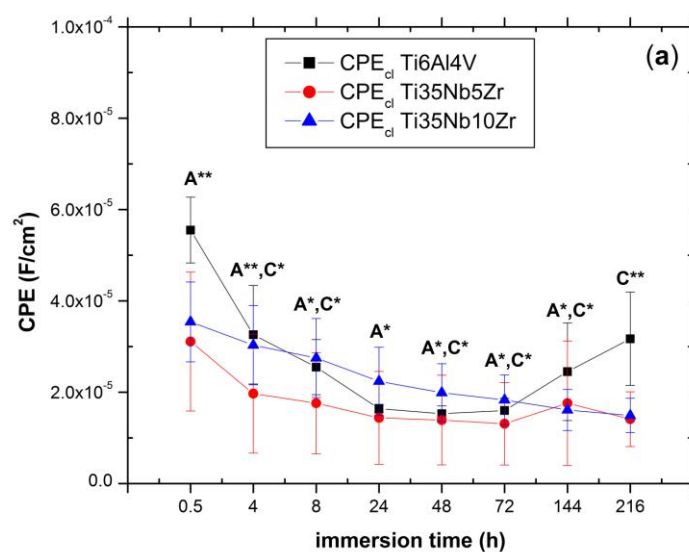
At the meanwhile,  $R_{cl}$  values were not statistical difference than the  $R_{pl}$  values in all considered periods for Ti35Nb5Zr ( $p>0.05$ ) while for Ti6Al4V,  $R_{cl}$  values were statistical higher than  $R_{pl}$  values at the periods 24h, 48h and 72h, showing that the resistances of the oxide films are not just attributed to the compact layer as reported before [27,29]. It is important to note that is ascribed to the porous layer the capacity of the alloys to osseointegrate [47].

In order to compare the total resistance ( $R_t$ ) of the double-layer alloys with  $R_{cl}$  of Ti35Nb10Zr, the sum of their  $R_{cl}$  and  $R_{pl}$  was accomplished [51], that are represented on Fig. 5c. No statistical difference was found among the three alloys ( $p>0.05$ ). The two-layer alloys  $R_t$  had the tendency to increase, reaching values around  $3.0 \times 10^6 \Omega \cdot \text{cm}^2$  similar to that of  $R_{cl}$  one-layer alloy stabilization value. This result suggested that the porous layers had a positive effect on Ti6Al4V and Ti35Nb5Zr passive layers resistance since the behaviour among the three alloys diverges to that verified on Fig. 5a. In other words, the  $R_{cl}$  of Ti35Nb10Zr was superior to  $R_{cl}$  of Ti35Nb5Zr and Ti6Al4V on almost all periods of time (Fig. 5a). However, there is no difference between  $R_{cl}$  of Ti35Nb10Zr and  $R_t$  of Ti35Nb5Zr and Ti6Al4V during the whole experiment (Fig. 5c).

Therefore, the combination action of  $R_{cl}$  and  $R_{pl}$  protects the two-layer alloys just as the  $R_{cl}$  protects the one-layer alloy.

Apparently, no resistance difference was found among the three alloys. However, it can be noted on Fig. 5 that the TiNbZr alloys results had large errors bars. Probably, the reason for that is the lack of homogeneity of the melted alloys. If the chemical composition is not homogeneous, it is expected a heterogeneous passive film.

Figure 6 shows the CPE results in function of immersion time. On Fig. 6a it is noted statistical difference of  $CPE_{cl}$  between the two-layer alloys for almost all periods of time, except at 0,5h and 24h. It shows that  $CPE_{cl}$  of Ti6Al4V was greater than Ti35Nb5Zr, showing that more amount of charge was accumulated on the Ti6Al4V-artificial saliva interface. Moreover, statistical difference was also found between  $CPE_{cl}$  of TiNbZr alloys, whereas Ti35Nb5Zr has better performance than Ti35Nb10Zr since its values were smaller, except at the last period, when no difference was found.



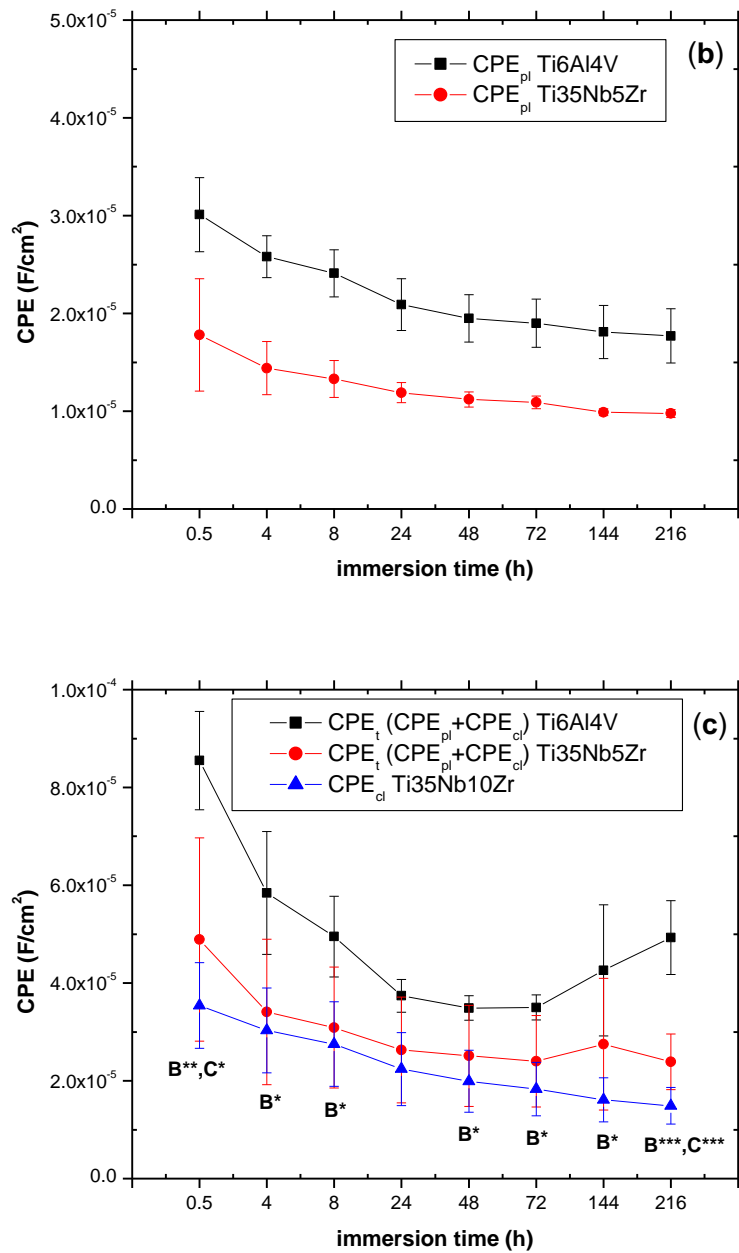


Figure 6 – Averages and standard deviations of (a)  $CPE_{cl}$ , (b)  $CPE_{pl}$  and (c)  $CPE_t$  ( $CPE_{pl} + CPE_{cl}$ ) and  $CPE_{cl}$  in function of time for Ti6Al4V, Ti35Nb5Zr and Ti35Nb10Zr. Statistical difference between Ti alloys in each period of time was calculated by ANOVA and Tukey's test (\* $p < 0.05$ , \*\* $p < 0.01$ , \*\*\* $p < 0.001$ ). (a) and (c) - letter **A** shows statistical difference of Ti35Nb5Zr vs. Ti35Nb10Zr, letter **B** shows statistical difference of Ti6Al4V vs. Ti35Nb10Zr and letter **C** shows statistical difference of Ti6Al4V vs. Ti35Nb5Zr. (a) - no statistical difference was found between Ti6Al4V vs. Ti35Nb10Zr alloys ( $p > 0.05$ ). (b) - no statistical difference was found among the three alloys. (c) - no statistical difference was found between Ti35Nb5Zr vs. Ti35Nb10Zr ( $p > 0.05$ ).



On Fig. 6b it is shown that the  $CPE_{pl}$  of both two layers alloys had the tendency to decrease and that there is no statistical difference between these alloys ( $p>0.05$ ).

Using the same principle of  $R_t$ , the total CPE was calculated ( $CPE_t$ ) by means of the sum of  $CPE_{cl}$  and  $CPE_{pl}$ . It was verified that the  $CPE_{cl}$  and  $CPE_t$  values had decreased in course of time and that TiNbZr alloys had alike behaviour ( $p>0.05$ ). This is interesting because indicates the long-term stability of the alloys passive film [35] and also confirms the improvement of the alloys behaviour in the course of time. The  $CPE_{cl}$  values of Ti35Nb10Zr were the smallest ones, showing statistical difference when comparing to Ti6Al4V at all periods, reaching  $1.50 \times 10^{-5} F/cm^2$  (Fig. 6c). Between the two-layer alloys, only at the first and last periods statistical difference was found, showing the negative influence of the porous layer that increased the total capacitance of Ti35Nb5Zr alloy.

Based on CPE data, the Ti35Nb10Zr alloy had better performance than Ti6Al4V and similar behaviour than Ti35Nb5Zr. These results can be related to oxides  $Nb_2O_5$  and  $ZrO_2$  formed on TiNbZr alloys in accordance to the literature as Nb and Zr oxides improve the passive film structure of Ti alloys [25,40,52,53].

The passive film behaviour of a metal can be related to its chemical composition [6,53,54]. It is known that the principal oxide formed on CP Ti is  $TiO_2$ , which has a recognized stability [5]. However, alloying elements can change its behaviour. For instance, V oxides can be formed on the passive film of Ti6Al4V [6]. Therefore, it can be prejudicial to the protective function of the

oxide film since Ti oxides are more resistant than V oxides [55,56]. For instance, V oxides can react with chloride ions present on aqueous solution promoting passive film dissolution of Ti6Al4V alloy [57].

Yu et al. [58] described that alloying additions of Nb and Zr to Ti lower its passive film dissolution in reducing acids. Besides, between Nb oxide and Ti oxide, the last is more susceptible to dissolution. Moreover, the alloying addition of Nb to Ti alloys leads to an eradication of anion vacancies caused by Ti suboxides. That is, Nb<sup>5+</sup> increase the number of oxygen ions, which nullify the anion vacancies making the film more homogeneous [56,59,60].

In addition, Al and Zr when added to Ti have the tendency to diffuse from the bulk material to form oxides on its surfaces [61] that contributes to a very protective passive film structure lowering the corrosion rate [62].

According to these characteristics, the amount of VO<sub>2</sub> or Nb<sub>2</sub>O<sub>5</sub> oxides on the composition of studied Ti alloys (Table 2) was not sufficient to make the Ti6Al4V resistance behaviour worse than TiNbZr alloys as they had similar behaviour. Probably, the amount of Al on Ti6Al4V compensated the prejudicial effect that V could have.

Moreover, the better capacitance behaviour of Ti35Nb10Zr than Ti6Al4V may be attributed to the more amount of Zr on its chemical composition as the more concentration of Nb<sub>2</sub>O<sub>5</sub> on its passive film. Another factor is the more compact passive film being more homogeneous contributes to less dissolution of the oxide film.

Therefore, despite all three alloys presented good corrosion resistance, Ti35Nb10Zr presented slightly better electrochemical behaviour than Ti6Al4V [27].

Although these TiNbZr are new alloys, the results can be compared to the literature by means of microstructure. The microstructures of the new alloys Ti35Nb5Zr and Ti35Nb10Zr are composed of  $\alpha+\beta$  phases and  $\beta$  phase, respectively [21]. Therefore, the results of this study are in accordance to the literature since it was described that near- $\beta$  Ti13Nb13Zr alloy had slightly better corrosion behaviour on EIS experiments than  $\alpha+\beta$  Ti6Al4V in Hanks's solution [27].

### **3.4. Clinical relevance**

It is worthy to mention that Ti and Ti alloys always corrode in physiologic media and that corrosion of metallic implants can adversely affect its biocompatibility and mechanical resistance. Metallic particles and ions released from implants can be harmful to the human body [13,14,16,18,19,39,63-66], affect osseointegration [16,17] and corrosion can cause devices failure [8,9]. Azevedo [67] verified that the failure of an oral maxillo-facial titanium plate, which occurred during use, was caused by a corrosion-fatigue mechanism. Hence, as the presence of Nb and Zr enhances the oxide layer, it is expected that a small amount of ions will be released from Ti35Nb10Zr alloy.

Many factors can influence on materials corrosion in oral environment as temperature, quantity and quality of saliva [68], biofilm [69], pH [43,70], proteins [31], fluoride content in oral hygiene products [71] and also, food and liquids

composition (physical and chemical properties) [8]. There are some evidences that  $\beta$  titanium alloys have similar or better behaviour than Ti6Al4V and CP Ti in contact to fluoride solution [72] and in contact to protein [31].

Considering all presented analysis, in general, the Ti35Nb10Zr alloy had a better behaviour than the Ti6Al4V alloy. Therefore, it is expected that the new Ti35Nb10Zr alloy will have the potential to be used in the dental field, in particular, in the manufacturing of dental implant-abutment sets as substitutes for the Ti6Al4V.

#### 4. Conclusions

The electrochemical behaviours of Ti<sub>35</sub>Nb<sub>5</sub>Zr, Ti<sub>35</sub>Nb<sub>10</sub>Zr and Ti<sub>6</sub>Al<sub>4</sub>V alloys were investigated in artificial saliva at 37°C. It can be concluded that:

- All three alloys exhibited potentials increased with time, i.e., passive film spontaneous formation that protects the alloys against corrosion.
- Ti<sub>35</sub>Nb<sub>5</sub>Zr and Ti<sub>6</sub>Al<sub>4</sub>V were described as two-layer passive film alloys and Ti<sub>35</sub>Nb<sub>10</sub>Zr as one-layer.
- Both three alloys had the same resistance behaviour and Ti<sub>35</sub>Nb<sub>10</sub>Zr had better capacitance behaviour than Ti<sub>6</sub>Al<sub>4</sub>V.
- When comparing the three materials, Ti<sub>35</sub>Nb<sub>10</sub>Zr alloy had higher corrosion resistance probably due to the Zr and Nb oxides formed on its surface together with its compact passive film.
- It is suggested that Ti<sub>35</sub>Nb<sub>10</sub>Zr alloy can be suitable alternative for dental implant application.

#### 5. Acknowledgements

The authors are grateful to Prof. Dr. Luís Augusto Rocha for his scientific support and to FAPESP (Fundação de Amparo a Pesquisa do Estado de São Paulo), Brazil and FCT (Fundação para a Ciência e a Tecnologia), Portugal, for their financial support. This work was conducted during a visiting scholar period at Universidade do Minho, sponsored by CAPES - Foundation Coordination for the Improvement of Higher Education Personnel, of the Ministry of Education, Brazil.

## 6. References

- [1] Saintrain MV and de Souza, EH. Impact of tooth loss on the quality of life. *Gerodontology* 2011; in press.
- [2] Yokoyama K, Ichikawa T, Murakami H, Miyamoto Y and Asaoka K. Fracture mechanisms of retrieved titanium screw thread in dental implant. *Biomaterials* 2002; 23:2459-2465.
- [3] Gilbert JL. Step-polarization impedance spectroscopy of implant alloys in physiologic solutions. *J Biomed Mater Res* 1998; 40:233-243.
- [4] Albrektsson T, Brånemark PI, Hansson HA, Kasemo B, Larsson K, Lindström I, McQueen DH and Skalak R. The interface zone of inorganic implants in vivo: Titanium implant in bone. *Ann Biomed Eng* 1983; 11:1-27.
- [5] Titanium and titanium alloys. In: Black J and Hasting G, editors. *Handbook of Biomaterial Properties*. London: Chapman and Hall, 1998. p. 179-200.
- [6] Milosev I, Antolic V, Minovic A, Cor A, Herman S, Pavlovcic V and Campbell P. Extensive metallosis and necrosis in failed prostheses with cemented titanium-alloy stems and ceramic heads, *J Bone Jt Surg Br* 2000; 82:352-357.
- [7] Olmedo DG, Duffó G, Cabrini RL and Guglielmotti MB. Local effect of titanium implant corrosion: an experimental study in rats. *Int J Oral and Maxillofac Surg* 2008; 37:1032-1038.
- [8] Chaturvedi TP. An overview of the corrosion aspect of dental implants (titanium and its alloys), *Indian J Dent Res* 2009; 20:91-98.

- [9] Rogers SD, Howie DW, Graves SE, Pearcy MJ and Haynes DR. In vitro human monocyte response to wear particles of titanium alloy containing vanadium or niobium. *J Bone Joint Surg Br* 1997; 79:311-315.
- [10] Choi MG, Koh HS, Kluess D, O'Connor D, Mathur A, Truskey GA, Rubin J, Zhou DXF and Paul Sung K-L. Effects of titanium particle size on osteoblast functions in vitro and in vivo. *PNAS* 2005; 102:4578-4583.
- [11] Mostardi RA, Kovacik MW, Ramsier RD, Bender ET, Finefrock JM, Bear TF and Askew MJ. A comparison of the effects of prosthetic and commercially pure metals on retrieved human fibroblasts: The role of surface elemental composition. *Acta Biomaterialia* 2010; 6:702-707.
- [12] Case CP, Langkamer VG, James C, Palmer MR, Kemp AJ, Heap PF and Solomon L. Widespread dissemination of metal debris from implants. *J Bone Jt Surg* 1994; 76B:701-712.
- [13] Perl DP and Moalem S. Aluminum and Alzheimer's disease, a personal perspective after 25 years. *J Alzheimers Dis* 2006; 9: 291-300.
- [14] Ngwa HA, Kanthasamy A, Anantharam V, Song C, Witte T, Houk R and Kanthasamy AG. Vanadium induces dopaminergic neurotoxicity via protein kinase Cdelta dependent oxidative signaling mechanisms: Relevance to etiopathogenesis of Parkinson's disease. *Toxicol Appl Pharmacol* 2009; 240:273-285.
- [15] Cremasco A, Messias AD, Esposito AR, Duek EADR and Caram R. Effects of alloying elements on the cytotoxic response of titanium alloys. *Mater Sci Eng C Mater Biol Appl* 2011; 31:833-839.

- [16] Rao S, Ushida T, Tateishi T, Okazaki Y and Asao S. Effect of Ti, Al, and V ions on the relative growth rate of fibroblasts (L929) and osteoblasts (MC3T3-E1) cells. *Biomed Mater Eng* 1996; 6:79–86.
- [17] Okazaki Y, Rao S, Ito Y and Tateishi T. Corrosion resistance, mechanical properties, corrosion fatigue strength and cytocompatibility of new Ti alloys without Al and V. *Biomaterials* 1998; 19:1197-1215.
- [18] Domingo JL. Vanadium: A review of the reproductive and developmental toxicity. *Reprod Toxicol* 1996; 10:175-182.
- [19] Siddiqi A, Payne AG, De Silva RK and Duncan WJ. Titanium allergy: could it affect dental implant integration? *Clin Oral Implants Res* 2011; 22:673-680.
- [20] Wang K. The use of titanium for medical applications in the USA. *Mater Sci Eng A Struct Mater* 1996; 213:134–137.
- [21] Ribeiro ALR, Caram Junior R, Cardoso FF, Fernandes Filho RB and Vaz LG. Mechanical, physical, and chemical characterization of Ti–35Nb–5Zr and Ti–35Nb–10Zr casting alloys. *J Mater Sci: Mater Med* 2009; 20:1629-1636.
- [22] Kim TI, Han JH, Lee IS, Lee KH, Shin MC and Choi BB. New titanium alloys for biomaterials: a study of mechanical and corrosion properties and cytotoxicity. *Biomed Mater Eng* 1997; 7:253-263.
- [23] Wang BL, Li L and Zheng YF. In vitro cytotoxicity and hemocompatibility studies of Ti-Nb, TiNbZr and Ti-Nb-Hf biomedical shape memory alloys. *Biomed Mater* 2010; 5:044102.



- [24] Ning C, Ding D, Dai K, Zhai W and Chen L. The effect of Zr content on the microstructure, mechanical properties and cell attachment of Ti-35Nb-xZr alloys. *Biomed Mater* 2010; 5:045006.
- [25] Choubey A, Basu B and Balasubramaniam R. Electrochemical behaviour of ti-based alloys in simulated human body fluid environment. *Trends Biomater Artif Organs* 2005; 18:64-72.
- [26] Assis SL, Wolyneć S and Costa I. Corrosion characterization of titanium alloys by electrochemical techniques. *Electrochim Acta* 2006; 51:1815–1819.
- [27] Assis SL and Costa I. Electrochemical evaluation of Ti13Nb13Zr, Ti6Al4V and Ti6Al7Nb alloys for biomedical application by long-term immersion tests. *Mater Corros* 2007; 58:329-333.
- [28] Alves VA, Reis RQ, Santos ICB, Souza DG, Gonçalves TF, Pereira-da-Silva MA, Rossi A and da Silva LA. In situ impedance spectroscopy study of the electrochemical corrosion of Ti and Ti–6Al–4V in simulated body fluid at 25 °C and 37 °C. *Corros Sci* 2009; 51:2473-2482.
- [29] Vasilescu E, Drob P, Raducanu D, Cinca I, Mareci D, Calderon Moreno JM, et al. Effect of thermo-mechanical processing on the corrosion resistance of Ti6Al4V alloys in biofluids. *Corros Sci* 2009; 51:2885-2896.
- [30] Figueira N, Silva TM, Carmezim MJ and Fernandes JCS. Corrosion behaviour of NiTi alloy. *Electrochim Acta* 2009; 54:921-926.
- [31] Khan MA, Williams RL, Williams DF. The corrosion behavior of Ti-6Al-4V, Ti-6Al-7Nb and Ti-13Nb-13Zr in protein solutions. *Biomaterials* 1999; 20:631-7.

- [32] Schiff N, Grosogogat B, Lissac M and Dalard F. Influence of fluoride content and pH on the corrosion resistance of titanium and its alloys. *Biomaterials* 2002; 23:1995-2002.
- [33] Barao VA, Mathew MT, Assunção WG, Yuan JC, Wimmer MA and Sukotjo C. Stability of cp-Ti and Ti6Al4V alloy for dental implants as a function of saliva pH - an electrochemical study. *Clin Oral Implants Res* 2011; in press.
- [34] Huang H-H. Effect of fluoride and albumin concentration on the corrosion behavior of Ti-6Al-4V alloy. *Biomaterials* 2003; 24:275-282.
- [35] Assis SL, Wolyneć S and Costa I. The electrochemical behaviour of Ti-13Nb-13Zr alloy in various solutions. *Mater Corros*, 2008; 59:739-743.
- [36] Robin A, Carvalho OAS, Schneider SG and Schneider S. Corrosion behavior of Ti-xNb-13Zr alloys in Ringer's solution. *Mat Corr* 2008; 59:929-33.
- [37] Fusayama T, Katayori T and Nomoto S. Corrosion of gold and amalgam placed in contact with each other. *J Dent Res* 1963; 42:1183-1197.
- [38] Okazaki Y, Tateishi T and Ito Y. Corrosion Resistance of Implant Alloys in Pseudo Physiological Solution and Role of Alloying Elements in Passive Films. *Mater Trans. JIM* 1997; 38:78-86.
- [39] Okazaki Y, Rao S, Asao S, Tateishi T, Katsuda S and Furuki Y. Effects of Ti, Al and V Concentrations on Cell Viability. *Mater Trans. JIM* 1998; 39:1053-1062.
- [40] Yu SY and Scully JR. Corrosion and passivity of Ti-13Nb-13Zr in comparison to other biomedical implant alloys. *Corrosion* 1997; 53:965-976.

- [41]Gordin DM, Gloriant T, Nemtoi Gh, Chelariu R, Aelenei N, Guillou A and Ansel D. Synthesis, structure and electrochemical behaviour of a beta Ti-12Mo-5Ta alloy as new biomaterial. *Mater Lett* 2005; 59:2936-2941.
- [42]Tait WS. An introduction to electrochemical corrosion testing for practicing engineers and scientists. USA: Pair O Docs Publication, 1994, p. 39.
- [43]Souza ME, Lima L, Lima CR, Zavaglia CA and Freire CM. Effects of pH on the electrochemical behaviour of titanium alloys for implant applications. *J Mater Sci Mater Med* 2009; 20:549-552.
- [44]Cvijović-Alagić I, Cvijović Z, Mitrović S, Panić V and Rakin M. Wear and corrosion behaviour of Ti-13Nb-13Zr and Ti-6Al-4V alloys in simulated physiological solution. *Corros Sci* 2011; 53:796-808.
- [45]González JEG and Mirza-Rosca JC. Study of the corrosion behaviour of titanium and some of its alloys for biomedical and dental implant applications. *J Electroanal Chem* 1999; 471:109-115.
- [46]Souto RM, Laz MM and Reis RL. Degradation characteristics of hydroxyapatite coatings on orthopaedic TiAlV in simulated physiological media investigated by electrochemical impedance spectroscopy. *Biomaterials* 2003; 24:4213-4221.
- [47]Lavos-Valereto IC, Wolyneć S, Ramires I, Guastaldi AC and Costa I. Electrochemical impedance spectroscopy characterization of passive film formed on implant Ti-6Al-7Nb alloy in Hank's solution. *J Mater Sci Mater Med* 2004; 15:55-59.

- [48]Oliveira NTC and Guastaldi AC. Electrochemical stability and corrosion resistance of Ti-Mo alloys for biomedical applications. *Acta Biomater* 2009; 5:399-405.
- [49]Mareci D, Chelariu R, Gordin D-M, Ungureanu G and Gloriant T. Comparative corrosion study of Ti-Ta alloys for dental applications. *Acta Biomater* 2009; 5:3625-3639.
- [50]Ibriş N and Mirza Rosca JC. EIS study of Ti and its alloys in biological media. *J Electroanal Chem* 2002; 526:53-62.
- [51]Marino CEB and Mascaro LH. EIS characterization of a Ti-dental implant in artificial saliva media: dissolution process of the oxide barrier. *J Electroanal Chem* 2004; 568:115-120.
- [52]Yu SY, Scully JR and Vitus CM. Influence of Niobium and Zirconium Alloying Additions on the Anodic Dissolution Behaviour of Activated Titanium in HCl Solutions. *J Electrochem Soc* 2001; 148:B68-78.
- [53]Guo WY, Sun J and Wu JS. Electrochemical and XPS studies of corrosion behaviour of Ti–23Nb–0.7Ta–2Zr–O alloy in Ringer's solution. *Mater Chem Phys* 2009; 113:816-820.
- [54]Milosev I, Kosec T and Strehblow H-H. XPS and EIS study of the passive film formed on orthopaedic Ti-6Al-7Nb alloy in Hank's physiological solution. *Electrochem Acta* 2008; 53:3547-3558.
- [55]Tamilselvi S, Murugaraj R and Rajendran N. Electrochemical impedance spectroscopic studies of titanium and its alloys in saline medium. *Mater Corros* 2007; 58:113-120.

- [56]Metikoš-Huković M, Kwokal A and Piljac J. The influence of niobium and vanadium on passivity of titanium-based implants in physiological solution. *Biomaterials* 2003; 24:3765-3775.
- [57]Ask M, Lausmaa J, Kasemo B. Preparation and surface spectroscopic characterization of oxide films on Ti6Al4V. *Appl Surf Sci* 1989; 35:283-301.
- [58]Yu SY, Scully JR, and Vitus CM. Influence of Niobium and Zirconium Alloying Additions on the Anodic Dissolution Behavior of Activated Titanium in HCl Solutions. *J Electrochem Soc* 2001; 148:B68-B78.
- [59]Kubaschewski O and Hopkins BE. *Oxidation of metals*. London: Butterworths, 1962.
- [60]Elliott SR. *The physics and chemistry of solids*. Chichester. England: Wiley, 1998.
- [61]Lopez MF, Gutierrez A and Jimenez JA. Surface characterization of new non-toxic titanium alloys for use as biomaterials. *Surf Sci* 2001; 482:300-305.
- [62]Sahu S, Palaniappa M, Paul SN and Roy M. Potentiodynamic behaviour of Ti alloys in physiological solution containing lubricant. *Mater Lett* 2010; 64:2-14.
- [63]Liu C, Leyland A, Bi Q and Matthews A. Corrosion resistance of multi-layered plasma-assisted physical vapour deposition TiN and CrN coatings. *Surf Coat Technol* 2001; 141:164-173.
- [64]Buly RL, Huo MH, Salvati E, Brien W and Bansal M. Titanium wear debris in failed cemented total hip arthroplasty. An analysis of 71 cases. *J Arthroplasty* 1992; 7:315-323.

- [65]Assem FL and Levy LS. A review of current toxicological concerns on vanadium pentoxide and other vanadium compounds: gaps in knowledge and directions for future research. *J Toxicol Environ Health B Crit Ver* 2009; 12:289-306.
- [66]Lemire J and Appanna VD. Aluminum toxicity and astrocyte dysfunction: a metabolic link to neurological disorders. *J Inorg Biochem* 2011; 105:1513-1517.
- [67]Azevedo CRF. Failure analysis of a commercially pure titanium plate for osteosynthesis. *Eng Fail Anal* 2003; 10:153-164.
- [68]Zavanelli RA, Guilherme AS, Pessanha-Henriques GE, Nóbilo MAA and Mesquita MF. Corrosion-fatigue of laser-repaired commercially pure titanium and Ti-6Al-4V alloy under different test environments. *J Oral Rehabil* 2004; 31:1029:1034.
- [69]Chang JC, Oshida Y, Gregory RL, Andres CJ, Barco TM and Brown DT. Electrochemical study on microbiology-related corrosion of metallic dental materials. *Biomed Mater Eng* 2003; 13:281-95.
- [70]Lindholm-Sethson B and Ardlin BI. Effects of pH and fluoride concentration on the corrosion of titanium. *J Biomed Mater Res A* 2008; 86:149-159.
- [71] Reclaru L and Meyer JM. Effects of fluorides on titanium and other dental alloys in dentistry. *Biomaterials* 1998; 19:85-92.
- [72] Kumar S, Sankara Narayanan TSN and Saravana Kumar S. Influence of fluoride ion on the electrochemical behaviour of  $\beta$ -Ti alloy for dental implant application. *Corros Sci* 2010; 52:1721-1727.

## **Capítulo 2**

### **On the tribocorrosion of new Ti35Nb5Zr and Ti35Nb10Zr alloys for dental applications: passive film vs. bulk behaviour**

Manuscrito redigido nas normas da revista científica Acta Biomaterialia.

On the tribocorrosion of new Ti35Nb5Zr and Ti35Nb10Zr alloys for dental applications: passive film vs. bulk behaviour

Ribeiro ALR<sup>a</sup>, Vaz LG<sup>b</sup>, Rocha LA<sup>c</sup>

<sup>a</sup> Departamento de Diagnóstico e Cirurgia, Faculdade de Odontologia de Araraquara, UNESP Univ Estadual Paulista, Araraquara, Brazil.

analuciaroselino@yahoo.com.br

<sup>b</sup> Departamento de Materiais Odontológicos e Prótese, Faculdade de Odontologia de Araraquara, UNESP Univ Estadual Paulista, Araraquara, Brazil.

lugervaz@foar.unesp.br

<sup>c</sup> Departamento de Engenharia Mecânica, Universidade do Minho, Guimarães, Portugal.

lrocha@dem.uminho.pt

Corresponding author: Ana Lúcia Roselino Ribeiro

Address: Rua Humaitá, 1680. FOAr-UNESP. 14801-903. Araraquara, SP, Brazil.

Phone number: +55 16 33016420

e-mail: analuciaroselino@yahoo.com.br



On the tribocorrosion of new Ti35Nb5Zr and Ti35Nb10Zr alloys for dental applications: passive film vs. bulk behaviour

### **Abstract**

Dental implants are under mechanical stresses and in contact with an aggressive environment. In such conditions, micro-movements occur between the implant and the adjacent bone leading to tribocorrosion degradation. Thus, the assessment of the degradation synergy resulting from combined action of corrosion and wear becomes important. The objective of this work was to investigate the tribocorrosion behavior of new Ti35Nb5Zr and Ti35Nb10Zr alloys, in comparison with the commercial available Ti6Al4V alloy. Tests were performed at different applied loads (50mN-1N) during 1200s in the reciprocating sliding configuration, in contact with an artificial saliva solution at 37°C. Experiments were carried out either in open-circuit potential or potentiostatic control mode. An alumina sphere was used as counterbody. Ti35Nb5Zr and Ti35Nb10Zr alloys presented better electrochemical behavior at low loads, probably due to their passive film properties. Ti6Al4V exhibited better performance during sliding at loads superior to 0.08N, when the bulk material was exposed for all three alloys. Therefore, bulk Ti6Al4V is more resistance to tribocorrosion.

**Key words:** dental implants, titanium alloys, tribocorrosion, artificial saliva

## 1. Introduction

There is a great concern in the medical field regarding the development of improved synthetic materials for the substitution, augmentation or regeneration of biological tissues. Regarding dental and maxillofacial applications, metallic, ceramic, polymeric materials and composites are used for a great number of medical rehabilitation processes.

Concerning metallic dental implants, the most used nowadays, their long-time success depends, among other characteristics, on the interaction between the material and the oral environment [1]. Those interactions always involve electrochemical reactions [2], mechanical stresses resulting from chewing, interfacial phenomena between implant-bone and/or implant-prosthesis and mechanical wear [3].

The evaluation of the combined action of mechanical wear and corrosion becomes important, since both wear and corrosion products might compromise the osseointegration process and result in adverse tissue reactions. For instance, metallic ions released can affect cell metabolism of fibroblast and odontoblasts [4,5] or can be systemically harmful if in contact with the bloodstream resulting in their accumulation in different organs [6]. Wear debris can induce local allergy in the oral tissue leading to edema and gingivitis [7,8]. Therefore, they can lead to implant failure.

Tribocorrosion is a degradation process that occurs simultaneously by mechanical and electrochemical mechanisms in the contact area between materials that slides together, when submerged in an aggressive medium [9,10]. Thus, tribocorrosion test appears as very important tool for the research of dental materials as it help in assessing the synergic effect caused by the

combined action of corrosion and wear, commonly present in dental implants and prosthesis [9-12]. Actually, the two phenomena can affect each other as wear can remove the metal passive film accelerating corrosion and corrosion can generate products, which can be able to influence the wear process [13,14].

Titanium (Ti) and the Ti6Al4V alloy are used for dental implant fabrication due to its good properties such as low density, high mechanical resistance and corrosion resistance which results from the existence of a surface protective oxide layer, i.e. a passive film (mainly TiO<sub>2</sub>) [15-17].

However, Ti and Ti alloys always suffer corrosion in the physiological environment. An investigation of osseointegration failed Ti dental implants by Arys et al. [18] showed that the composition and thickness of all implants oxide film were affected and Ti ions could be found on the tissue surrounding a failed implant. Additionally, Olmedo et al. [7] analyzed corroded implants retrieved from rats' tibiae and they observed scarce contact with bone, only in the areas with no surface damage. Furthermore, wear products when in contact to the tissues surrounding the implants can cause bone loss as found by Long e Rack [19] on a review of orthopedic alloys.

Regarding Ti6Al4V, its application as biomaterial is being discussed in the literature, because of the recognized toxicity of vanadium (V) and aluminium (Al) ions (released by corrosion) as they negatively affect fibroblasts and odontoblasts growth [17,20]. In fact, Al and V, when present in the brain are associated to the pathogenic of Alzheimer's disease and Parkinsonian dementia, neurophysiologic processes, respectively [21,22].

Therefore, efforts are being made towards the development of new Ti-based alloys with improved mechanical properties and biocompatibility through

the selection of alloying elements biologically less harmful as niobium (Nb) and zirconium (Zr). Niobium is a  $\beta$  phase-stabilizer resulting in improved mechanical properties, while Zr is a solid solution hardener. In addition, both elements are known to be non toxic [23-28].

Most of the studies on the tribocorrosion of biomaterials focus on the orthopedic function. Barril et al. [14,29] investigated the fretting-corrosion behaviour of Ti6Al4V in NaCl 0.9wt.%, using the ball-on-plate system against alumina ball. They observed that increase load and wear particles released from the contact area, which can oxidize, affected the electrochemical behaviour. Also, Martin et al. [30] investigated the influence of the microstructure on the tribocorrosion behaviour Ti6Al4V in contact with NaCl 1% solutions. They observed that the better corrosion behaviour was associated to  $\alpha+\beta$  alloy and that the higher hardness of martensitic contributed to less amount of debris. However, martensitic alloy had the most suitable microstructure when considering the synergic process. Concerning the effect of fluorides on the tribocorrosion behavior of Ti6Al4V, Sivakumar et al. [31] concluded that the addition of fluoride ions to artificial saliva influenced the repassivation of the alloy.

Wear behaviour of Ti13Nb13Zr alloys with different microstructures were evaluated under dry condition, Hank's solution and bovine serum. In general, the microstructure didn't influence the wear rate in dry condition. Moreover, the damage was increased for all alloys in the simulated body fluids, showing mainly abrasive wear [32]. In addition, More et al. [33] studied the tribocorrosion behaviour of Ti13Nb13Zr (6.5N applied load) against polyethylene in Hank's balanced salt solution. Polyethylene was transferred to the alloy, which had the

tendency to repassivate during sliding and at the end the potential was recovered, suggesting that the electrochemical and surfaces properties of the alloy were not significantly affected.

When comparing Ti6Al4V with the Ti13Nb13Zr alloy, Choubey et al. [34] described severe wear for both alloy under ball-on-plate tribocorrosion system at 10N applied load, in Hank's solution. Indeed, Cvijović-Alagić et al. [35] investigated the mechanical and electrochemical behaviour independently. They concluded that martensitic Ti23Nb13Zr had lower wear resistance (40N applied load) but higher corrosion resistance (Ringer's solution) than  $\alpha+\beta$  Ti6Al4V. Probably, this behaviour was observed because the oxides Nb<sub>2</sub>O<sub>5</sub> and ZrO<sub>2</sub> formed on TiNbZr are more corrosion resistant than the oxides Al<sub>2</sub>O<sub>3</sub> and VO<sub>2</sub> formed on Ti6Al4V surfaces [36-41] while the bulk metal has lower mechanical strength.

Nevertheless, no tribocorrosion study was found of Ti alloys from the TiNbZr system specifically to be used as dental material, considering effect of saliva. Also, no distinguish was made between the mechanical strength of the passive film and bulk metal of these alloys. All studies investigated the bulk metal since they were accomplished under loads that damaged the passive film.

In order to investigate the potential of new Ti alloys as biomaterial in dentistry, the purpose of this study was to evaluate the tribocorrosion behavior of the experimental alloys Ti35Nb5Zr and Ti35Nb10Zr at different applied loads (50mN-1N), in open circuit potential and at an anodic applied potential, in artificial saliva at 37°C. And, also, distinguish the contribution of passive film and bulk material to tribocorrosion. The results were compared with that observed in commercial Ti6Al4V alloy, tested in the same conditions.

## 2. Materials and methods

### 2.1. Alloys development and characterization

In this work, one commercial and two experimental alloys were evaluated. The Ti35Nb5Zr and Ti35Nb10Zr (wt%.) alloys were arc melted from pure metals, using a water-cooled copper hearth under an argon atmosphere as described before [42]. The obtained ingots were hot-forged in 10mm diameter bars and machined as discs (8mm diameter x 8mm height). Thereafter, the samples were heat treated at 1000°C for 1h and air cooled in order to relieve stress generated during the machining. The samples were cut vertically to be adapted to the tribocorrosion test. The  $\alpha+\beta$  Ti6Al4V alloy was machined as discs (25mm x 4.5mm) from acquired bar stock. As verified before [42], Ti35Nb5Zr has  $\alpha+\beta$  microstructure while Ti35Nb10Zr has  $\beta$  microstructure.

Afterwards, the samples were prepared for each analysis. The samples were mechanically polished with emery paper until #1200 and ultrasonically cleaned with propanol and distilled water and dried for Vickers's hardness test. For tribocorrosion tests and XPS analysis, they were mechanically polished with emery paper until #1200, ultrasonically cleaned with acetone, etched with Kroll's reagent (1ml HF, 5ml HNO<sub>3</sub>, 44ml distilled water), ultrasonically cleaned with hot distilled water (60°C) and dried using warm air, one day before the experiments in order to allow the formation of an oxide surface layer.

The Vickers's hardness test was carried out at 500gf for 15s, in 12 regions of each alloy (Micromet 2003, Buehler). The results were analyzed by variance analysis (ANOVA) and then Tukey's test ( $\alpha=0.05$ ).

The surface analysis was performed by X-ray spectroscopy (XPS) that was carried out at a pressure of less than  $10^{-6}$ Pa using a commercial spectrometer (UNI-SPECS UHV) to verify the changes in surface chemical composition of the alloys studied. The Mg K $\alpha$  line was used ( $h\nu = 1253.6$ eV) and the analyzer pass energy was set to 10eV. The inelastic background of the Nb 3d, Zr 3d, V 2p, Al 2p, Ti 2p, O 1s, C 1s, Ca 2p and P 2p electron core-level spectra was subtracted using Shirley's method. The composition of the near surface region was determined with an accuracy of  $\pm 10\%$  from the ratio of the relative peak areas corrected by Scofield's sensitivity factors of the corresponding elements. The spectra were fitted without placing constraints using multiple Voigt profiles. The width at half maximum (FWHM) varied between 1.1 and 2.1eV and the accuracy of the peak positions was  $\pm 0.1$ eV.

## **2.2. Tribocorrosion**

Tribocorrosion tests were carried out in a CETR tribometer (UMT-2, CETR, Campbell, California, USA) with the ball-on-plate configuration. It was used alumina balls (chemical inertness) of 10mm diameter against the three different titanium alloys in a reciprocating path (fresh alumina ball surface for each test). The experiments were performed with electrochemical measurements at open circuit potential ( $E_{\text{corr}}$ ) and at an applied anodic potential (Potentiostat: Reference 600, Gamry Instruments, Warminster, PA, USA). A saturated calomel electrode (SCE) was used as the reference electrode, a platinum (Pt) electrode as counter electrode and the Ti alloys as working electrode. The samples were masked with beeswax so that the exposed area was  $0.64\text{cm}^2$ . The electrolyte used was artificial saliva, similar to that described

by Fusayama et al. [43] (Table 1), 5.25 pH at 37°C. Before the tests, it was realized experiments with the alloys to know how much time they need to stabilize and it was established 1200s. Besides, during the experiments, the frictional coefficient was monitored in function of time.

Table 1 - Chemical composition of the artificial saliva solution (g/l)

NaCl	KCl	CaCl <sub>2</sub> .2H <sub>2</sub> O	Na <sub>2</sub> S.9H <sub>2</sub> O	NaH <sub>2</sub> PO <sub>4</sub> .2H <sub>2</sub> O	Urea
0.4	0.4	0.795	0.005	0.69	1

For the tribocorrosion tests at  $E_{corr}$ , it was applied different loads between 0.05 and 1N, with stroke length of 5mm at a frequency of 1Hz, during 1200s of reciprocating sliding. The direction of the sliding was perpendicular to the grinding grooves. The potential stabilization time was 1200s before and 1200s after the sliding.

For the tribocorrosion tests at anodic applied potential, the potential chosen was 500mV vs. SCE based on the polarization potentiodynamic curves (Fig. 1) to represent a passive potential of the alloys in the saliva solution. The tests parameters were similar to the previous experiment, except it was applied the loads 0.08N and 0.1N. The current stabilization time with applied potential was 500s before and 500s after the sliding. The amount of electric charge generated during these tests with potentiostatic control was calculated by integration of the curves (current x time) and the results were analyzed by variance analysis (ANOVA) and then Tukey's test ( $\alpha=0.05$ ).



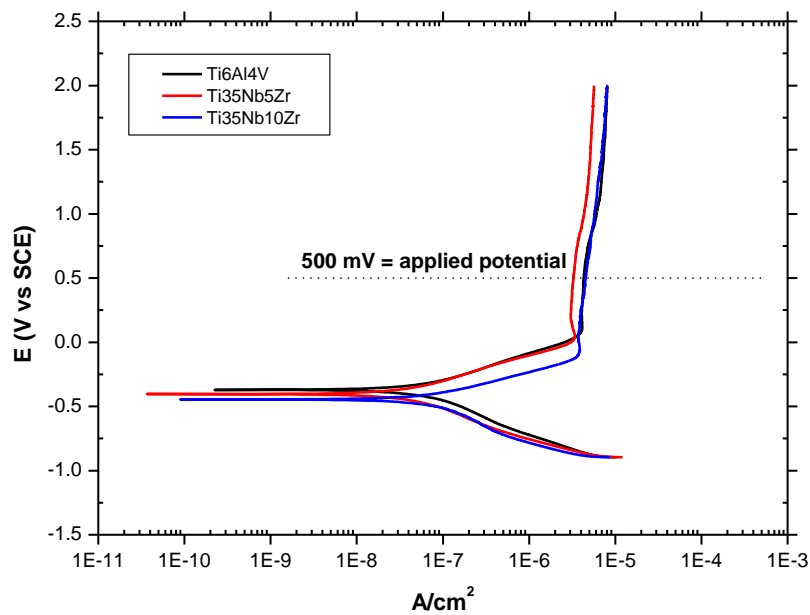


Figure 1 - Polarization potentiodynamic curves of Ti6Al4V, Ti35Nb5Zr and Ti35Nb10Zr alloys after 2h of open circuit potential, in artificial saliva solution at 37°C. Potential range from -0.9 to 2V, scan rate of 1mV/s.

The tests were made in triplicate to ensure reproducibility. Afterwards, the morphological analyses of the alloys wear tracks were realized in an Ultra-high resolution Field Emission Gun Scanning Electron Microscopy (FEG-SEM), NOVA 200 Nano SEM, FEI Company. And their chemical analyses were performed with the Energy Dispersive Spectroscopy (EDS) technique, using an Si(Li) detector, EDAX company. The alumina balls were analyzed by Scanning Electron Microscopy (SEM), Jeol-JSM.

### 3. Results and Discussion

#### 3.1. Tribocorrosion at open-circuit potential conditions

Figure 2 shows the tribocorrosion results obtained for the three alloys in open-circuit conditions, as a function of the applied loads 0.05N (Fig. 2a), 0.08N (Fig. 2b) and 1N (Fig. 2c). On the obtained curves ( $E_{\text{corr}} \times \text{time}$ ) it is possible to verify the electrochemical behaviour of the alloys. The potential ( $E_{\text{corr}}$ ) observed before the test starting represents the tendency to corrosion of the Ti alloys, in artificial saliva at 37°C. At that time, Ti alloys are in their passive state as passive film is formed on their surface. However, when the test starts, the alumina ball slides against the Ti alloys and can damage their passive film, concerning the applied force. When the passive film suffers damage, the Ti alloys became unprotected, therefore, the  $E_{\text{corr}}$  decreases. During the sliding, the alloys can suffer partial/total depassivation or repassivation and these behaviours can be interpreted by the changing of  $E_{\text{corr}}$ .

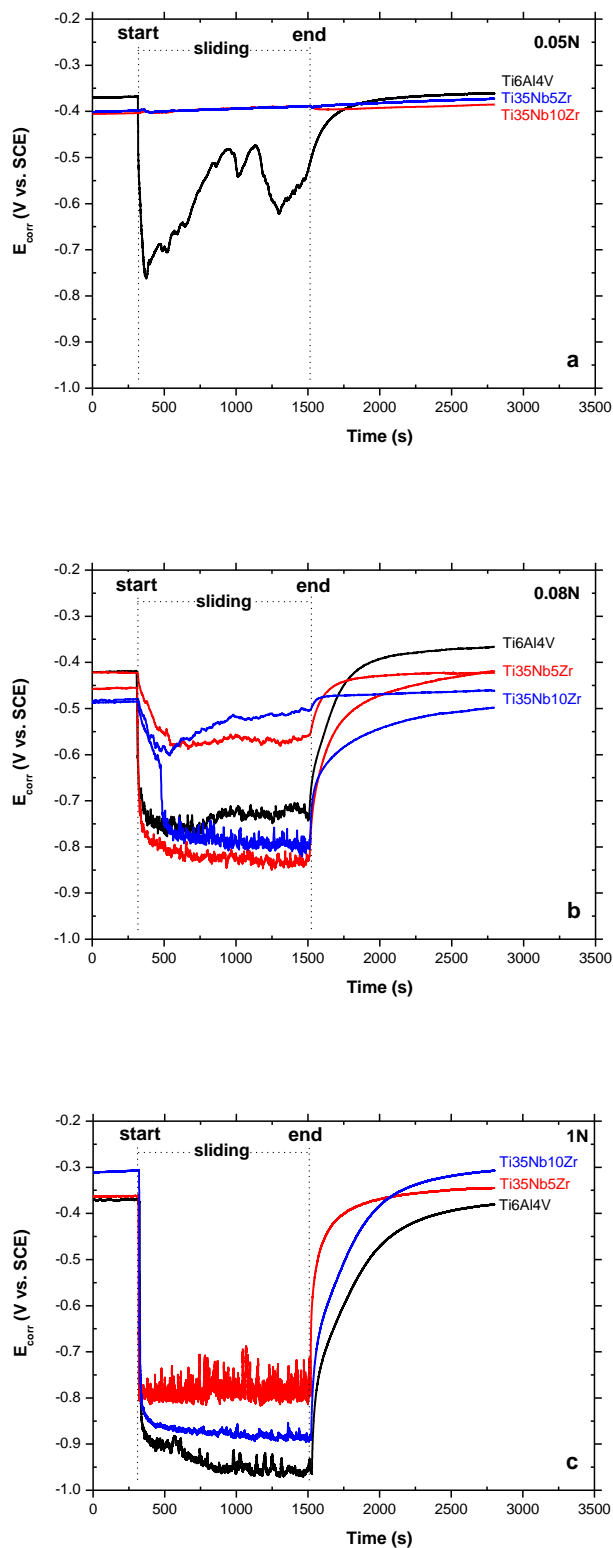


Figure 2 - Potential ( $E$ ) variation during tribocorrosion tests performed at open circuit potential in artificial saliva at 37°C with 5mm stroke, 1Hz, at different applied loads (a) 0.05N, (b) 0.08N and (c) 1N. Sliding starts at 300s.

On Fig. 2a it is noted that the  $E_{\text{corr}}$  of Ti6Al4V had a drop when sliding started of about 300mV. Nevertheless, during sliding a slight continuous increase in electrochemical potential can be observed with some intermittent drops. At the end of the test, a rapid repassivation occurred. However, no significant variation of potential could be observed for the Ti35Nb5Zr and Ti35Nb10Zr.

When the applied load increase to 0.08N, the alloys behaviour changed as can be seen on Fig. 2b. It is observed the Ti6Al4V  $E_{\text{corr}}$  rapid decrease, approximately 300mV, as the test started and small fluctuation of the potential during sliding. Rapid repassivation occurred with the test ending. At this point, both TiNbZr alloys presented two distinct behaviours as can be seen from the curves on Fig. 2b. When the test started, the Ti35Nb5Zr  $E_{\text{corr}}$  either had a decrease of approximately 350mV, having the same behaviour of Ti6Al4V, or the potential decreased only 150mV. At the end, the film rapidly repassivated. The same happened for Ti35Nb10Zr, but with low changing of  $E_{\text{corr}}$ , which decreased approximately 300mV or 100mV, in which case the potential had the tendency to repassivate during the sliding.

As the applied load increase to 1N, all three alloys had similar behaviour, i.e., as soon as the sliding started, the  $E_{\text{corr}}$  had a drop around 400mV, maintaining this value with small fluctuation during the test. At the end, the passive films were completely recovered.

The fluctuation of  $E_{\text{corr}}$  during the tribocorrosion tests is due to the depassivation and repassivation of the passive film [31]. It is explained by the fact that the test is a reciprocating sliding and, when the alumina ball touches

the material it removes the passive film and a depassivation happens and until the ball comes back, there is time for the material to repassivate.

For all alloys, the final  $E_{\text{corr}}$ , measured after the repassivation, were similar or even higher than the initial ones, before the test starts. And they were recovered as soon as the sliding was ceased, independently of the applied load. Hence, the newly passive films formed after sliding had characteristics relatively similar to the original ones [12]. Probably, the reason for some final  $E_{\text{corr}}$  being greater than initial ones is that the passive oxide films can grow during the test [10] in the areas not submitted to sliding [33]. It is worthy to say that the potential measured during sliding is related to the galvanic coupling of the two distinct areas of the alloys, the passive film of the unworn areas and the bare metal of the worn area, which suffers depassivation and repassivation during the test and can be exposed to the artificial saliva [10].

Observing the different behaviours of each alloy at the different applied loads, it is possible to verify that Ti6Al4V had a partially depassivation at 0.05N and 0.08N and a totally depassivation at 1N. At 0.05N, repassivation occurred during the test. However, TiNbZr alloys showed different behaviours. At 0.05N, the passive films had no damage while at 1N, they were completely removed. Moreover, at 0.08N it was observed a transitional area of the electrochemical behaviour, probably because the passive film starts to break at this load.

Therefore, at low loads the Ti alloys behaviour can be explained by their passive film characteristics. Table 2 shows the composition of the passive film for all alloys by means of percentage calculated from the XPS results. As can be seen, the passive film was mainly formed of  $\text{TiO}_2$  on Ti6Al4V surfaces and of  $\text{TiO}_2$  and  $\text{Nb}_2\text{O}_5$  on TiNbZr surfaces. As on the tribocorrosion test the corrosion

and mechanical wear act simultaneously, it is important to clarify the behaviour of the oxides under both conditions.

Table 2 - Percentage of oxides on Ti6Al4V, Ti35Nb5Zr and Ti35Nb10Zr passive film, calculated from XPS results

	Ti6Al4V	Ti35Nb5Zr	Ti35Nb10Zr
TiO <sub>2</sub>	86.53%	59.38%	39.80%
Al <sub>2</sub> O <sub>3</sub>	11.60%	-	-
VO <sub>2</sub>	1.87%	-	-
Nb <sub>2</sub> O <sub>5</sub>	-	36.64%	52.07%
ZrO <sub>2</sub>	-	3.98%	8.13%

The principal oxide formed on Ti is the TiO<sub>2</sub>, which has a recognized resistance to corrosion in artificial saliva [15]. However, on Ti alloys, the alloying elements can have a decisive role on the passive film behaviour. For instance, on Ti6Al4V alloy, V oxides were formed but they have less resistance than Ti oxides [36,37]. In addition, V oxides can react with chloride ions present on the artificial saliva promoting dissolution of the passive film [38]. On the other hand, on TiNbZr, Nb oxides is formed and they have less susceptible to dissolution than Ti oxides [39]. Therefore, the artificial saliva could be more deleterious to Ti6Al4V than to TiNbZr alloys passive films.

Moreover, the Ti alloy passive film composed of Nb oxides is more homogeneous because the Nb<sup>5+</sup> increases the amount of oxygen ions, which nullify the anion vacancies present on Ti oxide film [37,40,41]. In addition, the

$\text{Nb}_2\text{O}_5$  is harder than  $\text{TiO}_2$  [44]. Hence, it can contribute to the passive film mechanical strength.

These cited properties can explain the better behaviour of TiNbZr alloys than Ti6Al4V. Consequently, the passive films formed on the new alloys are more corrosion and mechanical resistance.

On the other hand, at 1N applied load the passive film was totally removed and all alloys showed similar electrochemical behaviour.

Figure 3 shows the micrographs of the wear tracks after sliding at 1N applied load. The FEG-SEM images of major resolution (Fig. 3a,b,c) show the general aspect of the wear tracks. It is possible to note the similarity among the wear tracks, showing surface scratches that indicate wear by abrasion [33,35].

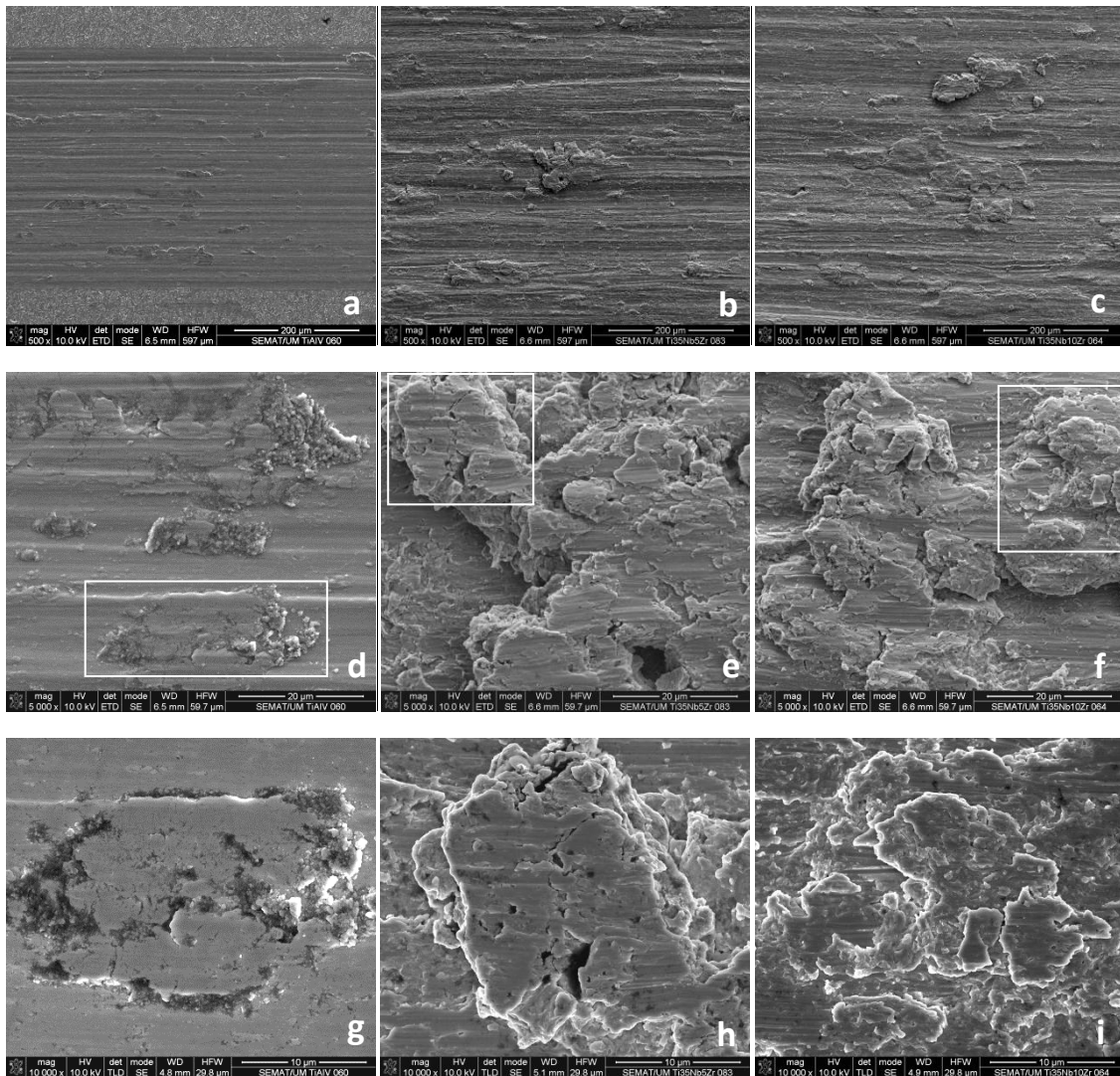


Figure 3 - FEG-SEM images of the alloys Ti6Al4V (left side), Ti35Nb5Zr (middle) and Ti35Nb10Zr (right side) found after tribocorrosion tests performed at OCP in artificial saliva at 37°C with 5mm stroke, 1Hz, at 1N during 1200s. The first micrographs (a, b and c) (500x) show the worn and unworn surfaces, followed by images (d, e and f) (5000x) of the wear tracks with greater amplitude showing the surface scratchers and debris, and the images (g, h and i) (10000x) regarding the squares, showing the debris in detail.



The first micrographs (a, b and c) show the worn and unworn surfaces, followed by images (d, e and f) of the wear tracks with greater amplitude showing the surface scratchers and debris, and the images (g, h and i) regarding the squares, showing the debris in detail.

On Fig. 3a it is possible to see the interface between the worn and unworn surfaces of the Ti6Al4V different from TiNbZr alloys, Fig. 3b and Fig. 3c. Hence, the wear scar of Ti6Al4V was thinner than the other two alloys. This can be related to the hardness values, presented on Table 3. Ti6Al4V presented the higher hardness value that means more resistance to plastic deformation so less contact between the alumina ball and the material [30]. Although the hardness values between TiNbZr alloys are different, they showed similar wear tracks.

Table 3 – Vickers hardness (SD) of Ti6Al4V, Ti35Nb5Zr and Ti35Nb10Zr

Alloys	Hardness HV (SD)*
Ti6Al4V	345.05 (15.71) <sup>a</sup>
Ti35Nb5Zr	330.20 (17.07) <sup>b</sup>
Ti35Nb10Zr	185.84 (10.66) <sup>c</sup>

\*Different lower cases in columns show hardness statistical difference by Tukey's test (Ti6Al4V vs Ti35Nb5Zr -  $p < 0.05$ , Ti6Al4V vs Ti35Nb10Zr and Ti35Nb5Zr vs Ti35Nb10Zr -  $p < 0.001$ ).

Figures 3d-f show the plastic deformation of the Ti alloys with longitudinal scratches aligned to the sliding direction, which can be associated to the presence of wear debris in the contact zone [45]. Figures 3g-i present the debris, with more magnitude, that were adhered to the surface and did not

release with the ultrasonically cleaning prior to FEG-SEM analysis. It is observed signs of wear by adhesion and fatigue, the latter characterized by perpendicular cracks on the debris, which can be released and act as third bodies.

These debris were formed from the counterbody rubbing against the tested Ti alloys, leading to the release of these metal particles. Thus, the abrasive morphology was caused by wear particles that were sufficiently strain hard to penetrate the material as related by Magaziner et al. [46] on Ti6Al4V wear surfaces.

In fact, the third bodies can be adhered on the counterbody or be spread between the metal and counterbody. Consequently, they can be oxidized and then modify the electrochemical measurements [47]. The debris can also be ejected from the contact during the sliding [14] and remove the oxide protective layer around the track, increasing the corrosion [45]. Therefore, the third bodies can also influence the potential variation during sliding at the worn and unworn areas. Probably, as the load increases, more particles are detached from the metals surfaces, that can influence negatively on the alloys tribocorrosion behavior.

Figures 4a-c present the EDS analysis of the debris. It was not found indication of  $\text{Al}_2\text{O}_3$  transferred from the alumina ball on the wear tracks on the EDS spectra of any Ti alloy. However, macroscopically and microscopically it was observed metal adhered on the alumina balls used on the corresponded tests as seen on SEM images on Fig. 5. More amount of metal was found on alumina spheres used against TiNbZr alloys than the ones used against Ti6Al4V, as can be seen on Fig. 5a-c.

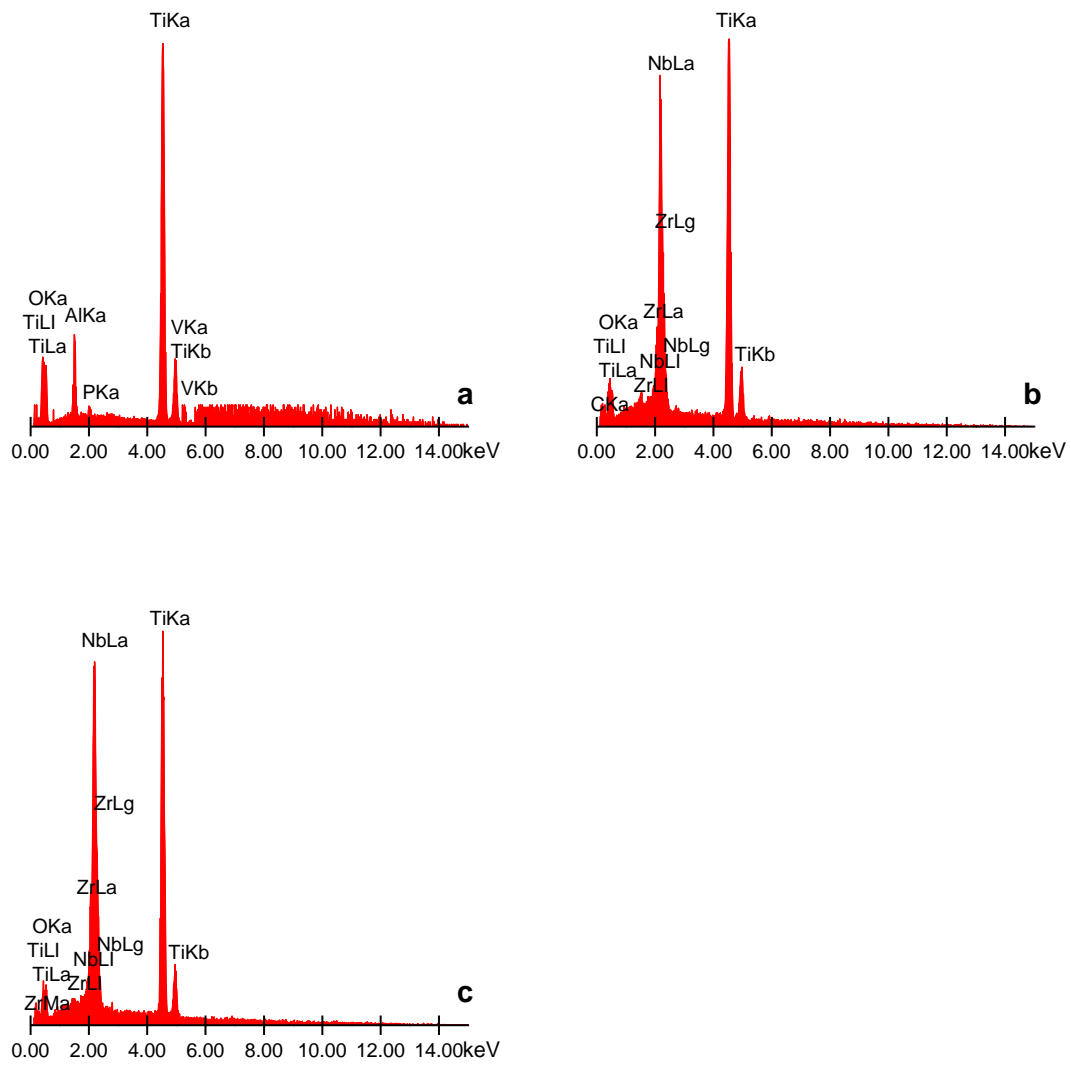


Figure 4 - EDS spectra of the debris of Ti6Al4V (a), Ti35Nb5Zr (b) and Ti35Nb10Zr (c).

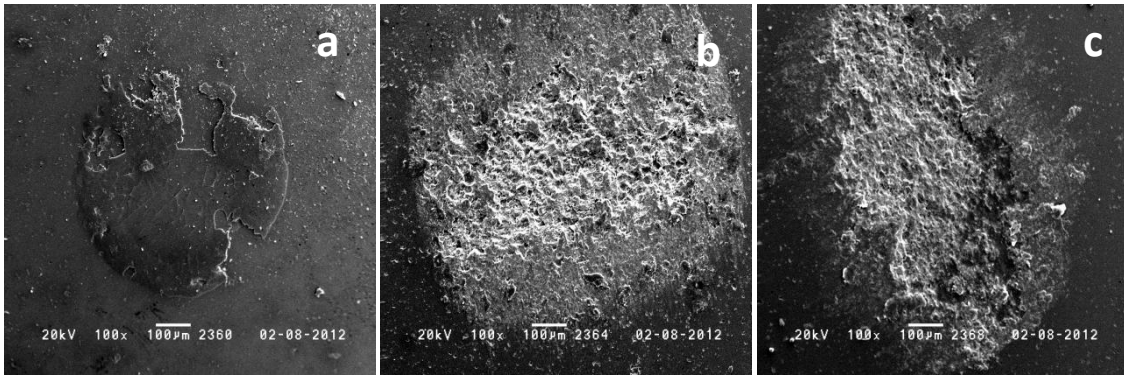


Figure 5 - SEM images (100x) of alumina balls with metal adhered, after tribocorrosion tests performed at open circuit potential in artificial saliva at 37°C with 5mm stroke, 1Hz, at 1N during 1200s. (a) Ti6Al4V, (b) Ti35Nb5Zr and (c) Ti35Nb10Zr.

Simultaneously to the potential variation, an oscillation of the coefficient of friction (COF) occurs. Figures 6a-c show the  $E_{\text{corr}}$  and COF at the same graphic for each Ti alloy at 0.1N applied load. The COF started to increase as the  $E_{\text{corr}}$  decreased and the oscillation of COF is in accordance to the oscillation of  $E_{\text{corr}}$ , which can be related to the third bodies' formation as described before. Consequently, the third bodies can also influence the COF when accumulated in the contact region between the Ti alloys and the counterbody [12]. Moreover, it can be seen on these graphs that the 0.1N applied load was able to damage the passive film of all three alloys.

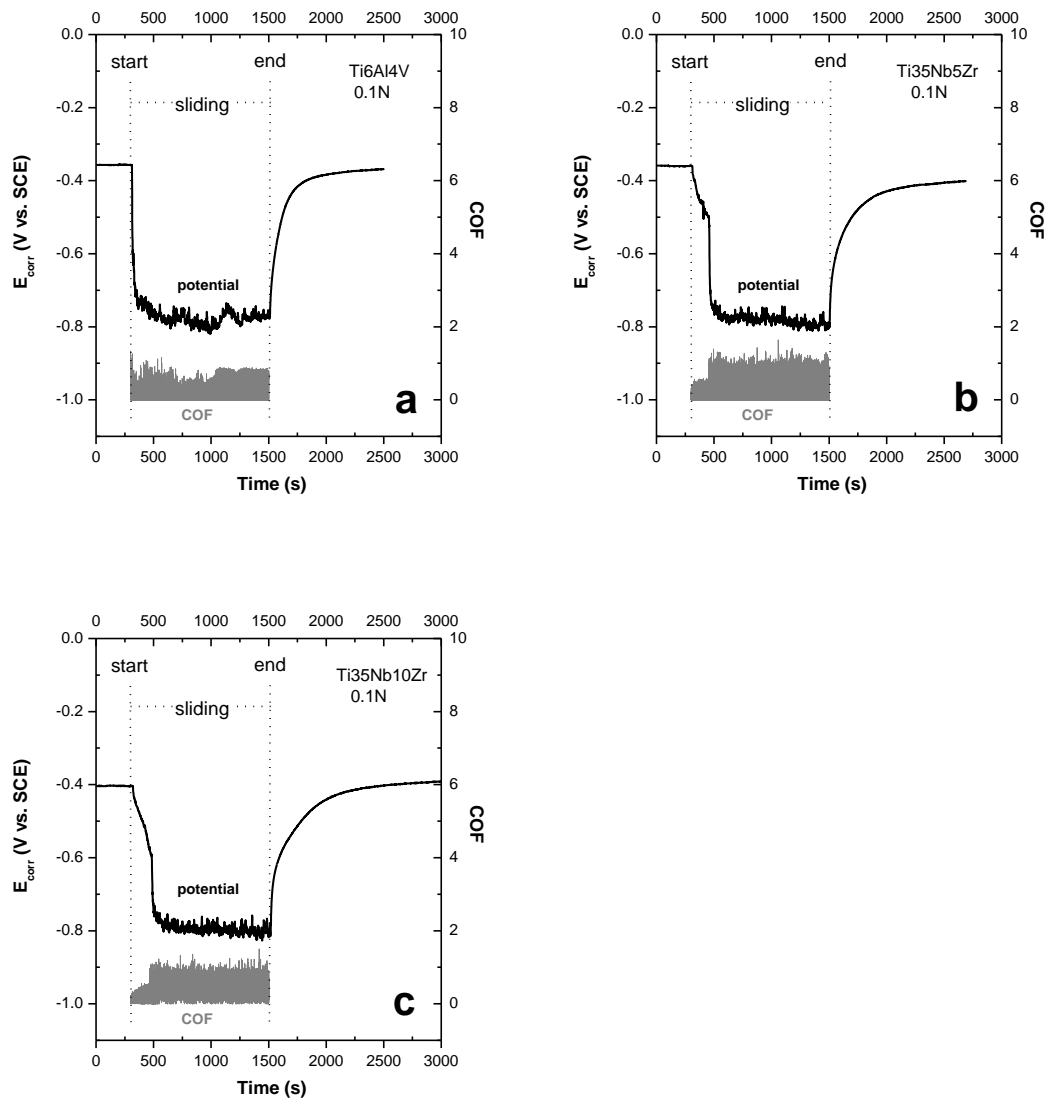


Figure 6 - Potential ( $E$ ) and coefficient of friction (COF) as a function of time for Ti6Al4V (a), Ti35Nb5Zr (b) and Ti35Nb10Zr (c) during 1200s of sliding at 0.1N applied load.

### 3.2. Tribocorrosion with potentiostatic control

Tribocorrosion tests were performed at an applied anodic potential (500mV) so that the passive film characteristics could be monitored during the sliding. Figure 7 presents the variation of current (A) as a function of time (s), during sliding at 0.1N applied load. As can be seen, when the potential was applied ( $t=0s$ ) the current tended to zero. It represents the passive film stabilization. Moreover, as the load was applied, the current suddenly increased to anodic values characterizing an oxidation of the bare metal in contact to the artificial saliva. That is, ions are released to maintain the potential at 500mV. In sequence, the anodic current oscillated during the rubbing because of the alternating action of the ball [30]. The current increase is proportional to the damage of the passive film. At the unloading, a steep decrease of the current showed the repassivation of the passive film on the worn area [10]. Therefore, the amount of ions released relies on the process of depassivation and repassivation of the oxide film. Thus, the measured current at an applied potential during sliding is referent to the performance of the metal in the wear track [13].

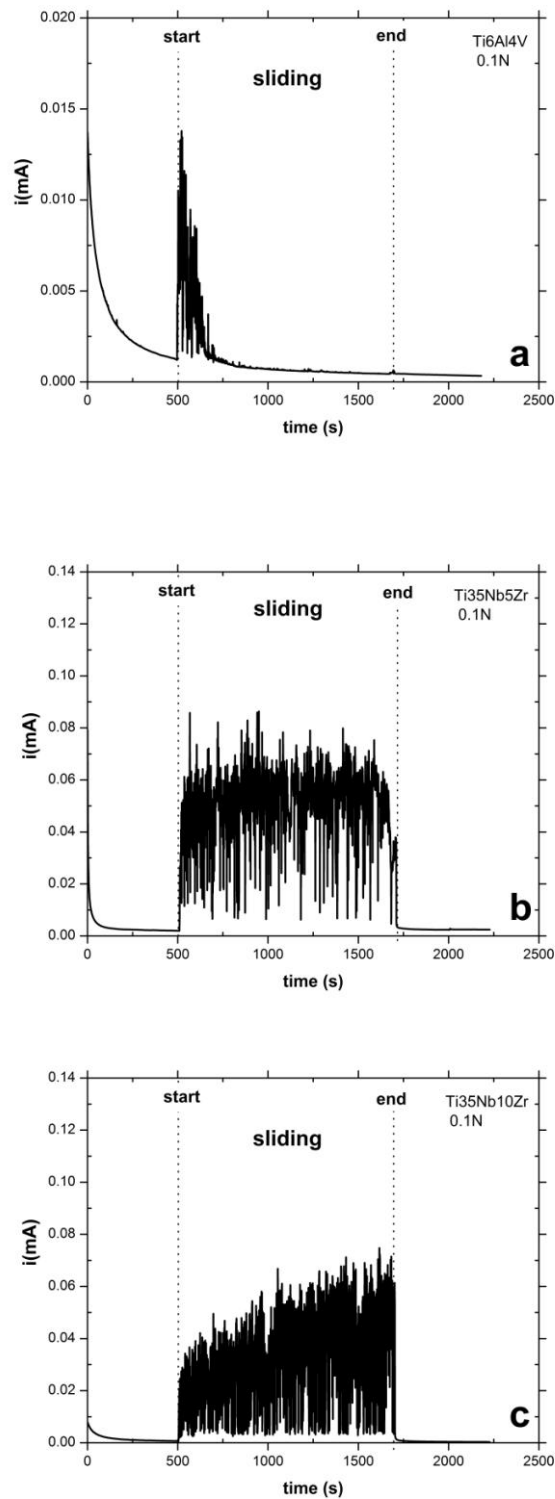


Figure 7 - Current (A) variation as a function of time for Ti6Al4V (a), Ti35Nb5Zr (b) and Ti35Nb10Zr (c) during 1200s of sliding performed at applied anodic potential in artificial saliva at 37°C with applied load of 0.1N, 5mm stroke, 1Hz. Sliding starts at 500s.

At this point, it is possible to verify that the alloys had different behaviours. Ti6Al4V (Fig. 7a) present less current oscillation than TiNbZr alloys (Fig. 7a e b), during sliding at 0.1N.

Moreover, the electrochemical response of the material to the sliding contact can be evaluated through the electric charge generated during the sliding contact. This electric charge was assessed integrating the current curves or calculating the area under the curves (Fig. 7a-c).

Figure 8 presents the amount of electric charge transferred from each alloy as a function of applied load, when under tribocorrosion process at 500mV applied potential. As can be seen, the Ti6Al4V released less electric charge than TiNbZr, independently of the applied load. No difference was found between the amount of charge generated from Ti35Nb5Zr and Ti35Nb10Zr.

Considering that the passive films for all three alloys were damaged during sliding at 0.01N applied load at open circuit potential, the electrochemical contribution present on Fig. 8 at 0.1N is related to the bulk alloys. Therefore, the bulk Ti6Al4V had better behaviour than TiNbZr alloys.



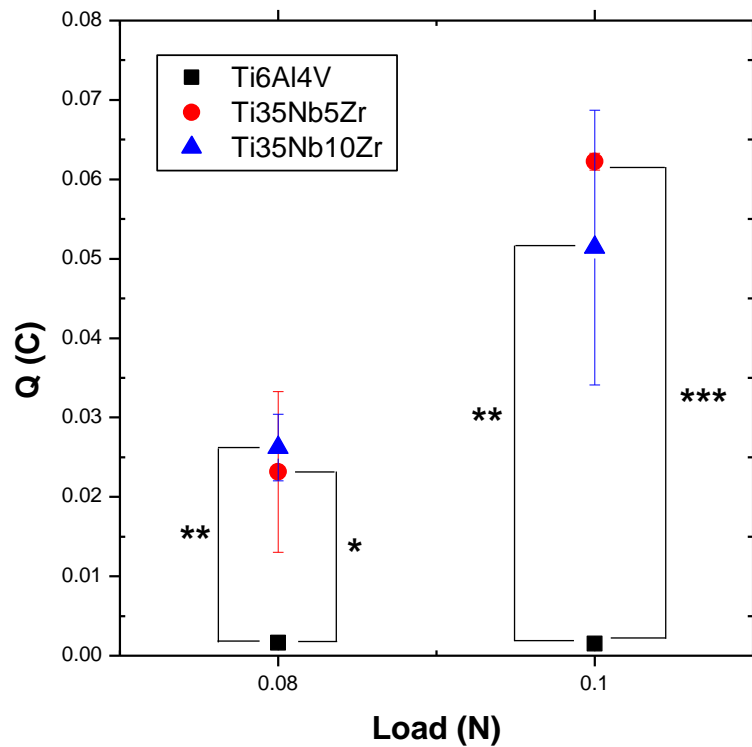


Figure 8 – Amount of electric charge generated after tribocorrosion test at potentiostatic control (500mV), in function of applied load. Statistical difference between Ti alloys in each load was calculated by ANOVA and Tukey's test (\* $p < 0.05$ , \*\* $p < 0.01$ , \*\*\* $p < 0.001$ ). No statistical difference was found between Ti35Nb5Zr and Ti35Nb10Zr.

Even though the microstructural composition of TiNbZr alloys are different since Ti35Nb5Zr presents  $\alpha$  and  $\beta$  phases and Ti35Nb10Zr, only  $\beta$  phase, no significance difference were noticed on the tribocorrosion behaviour, independently of the applied load or potential condition.

Although differences among the alloys were exhibited, at the sliding end, the potential reached back the values before the test for all tribocorrosion conditions studied for all three alloys. It indicated that the passive films were

repaired on the worn areas. Indeed, the rapid repassivation leads to a less amount of released metal ions into the body.

Furthermore, on the present investigation, Ti6Al4V exhibited higher hardness values, thinner wear scar and less amount of released charge, therefore, presented the better bulk behavior. However, Ti35Nb5Zr and Ti35Nb10Zr alloys presented the better electrochemical behavior at low loads, confirming that the passive formed on their surfaces had better behaviour.

Consequently, it is suggested to growth the oxide film of the new TiNbZr alloys by anodization expecting their better performance with the advantage of its biocompatibility.

#### **4. Conclusion**

In this study, the tribocorrosion behavior of titanium alloys was investigated under different loads and potential condition, in artificial saliva at 37°C. The following conclusions can be drawn from the results.

- All alloys showed repassivation of the passive films after unloading at all considered conditions.
- The electrochemical behavior was sensitive to the applied load;
- Ti35Nb5Zr and Ti35Nb10Zr passive films had better behaviour at low loads than Ti6Al4V;
- Bulk Ti6Al4V had better behaviour than TiNbZr alloys.

#### **5. Acknowledgements**

The authors are grateful to the financial support of FAPESP (Fundação de Amparo a Pesquisa do Estado de São Paulo), Brazil and FCT (Fundação para a Ciência e a Tecnologia), Portugal. This work was conducted during a visiting scholar period at Universidade do Minho, sponsored by CAPES - Foundation Coordination for the Improvement of Higher Education Personnel, of the Ministry of Education, Brazil.

## 6. References

1. Fathi MH, Salehi M, Saatchi A, Mortazavi V, Moosavi SB. In vitro corrosion behavior of bioceramic, metallic, and bioceramic-metallic coated stainless steel dental implants. *Dent Mater* 2003;19:188-98.
2. Molina C, Nogués L, Martinez-Gomis J, Peraire M, Salsench J, Sevilla P et al. Dental casting alloys behaviour during power toothbrushing with toothpastes of various abrasivities. Part II: corrosion and ion release. *J Mater Sci Mater Med* 2008;19:3015-3019.
3. Karov J, Hinberg I. Galvanic corrosion of selected dental alloys. *J Oral Rehabil* 2001;28:212-219.
4. Choi MG, Koh HS, Klues D, O'Connor D, Mathur A, Truskey GA, Rubin J, Zhou DXF and Paul Sung K-L. Effects of titanium particle size on osteoblast functions in vitro and in vivo. *PNAS* 2005;102:4578-4583.
5. Mostardi RA, Kovacic MW, Ramsier RD, Bender ET, Finefrock JM, Bear TF and Askew MJ. A comparison of the effects of prosthetic and commercially pure metals on retrieved human fibroblasts: The role of surface elemental composition. *Acta Biomater* 2010;6:702-707.
6. Case CP, Langkamer VG, James C, Palmer MR, Kemp AJ, Heap PF and Solomon L. Widespread dissemination of metal debris from implants. *J Bone Jt Surg* 1994;76B:701-712.
7. Olmedo DG, Duffó G, Cabrini RL and Guglielmotti MB. Local effect of titanium implant corrosion: an experimental study in rats. *Int J Oral and Maxillofac Surg* 2008;37:1032-1038.
8. Chaturvedi TP. An overview of the corrosion aspect of dental implants (titanium and its alloys), *Indian J Dent Res* 2009;20:91-98.

9. Landolt D, Mischler S, Stemp M. Electrochemical methods in tribocorrosion: a critical appraisal. *Electrochim Acta* 2001;46:3913-3929.
10. Mischler S. Triboelectrochemical techniques and interpretation methods in tribocorrosion: A comparative evaluation. *Tribol Int* 2008;41:573-583.
11. Fernandes AC, Vaz F, Ariza E, Rocha LA, Ribeiro ARL, Vieira AC, Riviere JP, Pichon L. Tribocorrosion behaviour of plasma nitrided and plasma nitrided + oxidised Ti6Al4V alloy. *Surf Coat Technol* 2006;200:6218-6224.
12. Vieira AC, Ribeiro AR, Rocha LA, Celis AP. Influence of pH and corrosion inhibitors on the tribocorrosion of titanium in artificial saliva. *Wear* 2006;261:994-1001.
13. Ponthiaux P, Wenger F, Drees D, Celis JP. Electrochemical techniques for studying tribocorrosion processes. *Wear* 2004;256:459-468.
14. Barril S, Debaud N, Mischler S, Landolt D. A tribo-electrochemical apparatus for in vitro investigation of fretting-corrosion of metallic implant materials. *Wear* 2002;252:744-754.
15. Black J and Hasting G. Titanium and titanium alloys. In: *Handbook of Biomaterial Properties*. Springer-Verlag/Chapman & Hall Ltd. London; 1998. p 590.
16. Okazaki Y, Tateishi T and Ito Y. Corrosion Resistance of Implant Alloys in Pseudo Physiological Solution and Role of Alloying Elements in Passive Films. *Mater Trans, JIM* 1997;38:78-84.
17. Okazaki Y, Rao S, Asao S, Tateishi T, Katsuda S and Furuki Y. Effects of Ti, Al and V Concentrations on Cell Viability. *Mater Trans, JIM* 1998;39:1053-1062.

18. Arys A, Philippart C, Dourov N, He Y, Le QT, Pireaux JJ. Analysis of titanium dental implants after failure of osseointegration: combined histological, electron microscopy, and X-ray photoelectron spectroscopy approach. *Biomed Mater Res* 1998;43:300-312.
19. Long M, Rack HJ. Titanium alloys in total joint replacement—a materials science perspective. *Biomaterials* 1998;19:1621-1639.
20. Rao S, Ushida T, Tateishi T, Okazaki Y, Asao S. Effect of Ti, Al, and V ions on the relative growth rate of fibroblasts (L929) and osteoblasts (MC3T3-E1) cells. *Biomed Mater Eng* 1996;6:79-86.
21. Perl DP, Moalem S. Aluminum and Alzheimer's disease, a personal perspective after 25 years. *J Alzheimers Dis* 2006;9:291-300.
22. Ngwa HA, Kanthasamy A, Anantharam V, Song C, Witte T, Houk R, Kanthasamy AG. Vanadium induces dopaminergic neurotoxicity via protein kinase Cdelta dependent oxidative signaling mechanisms: Relevance to etiopathogenesis of Parkinson's disease. *Toxicol Appl Pharmacol* 2009;240:273-285.
23. Niinomi M. Fatigue performance and cyto-toxicity of low rigidity titanium alloy, Ti–29Nb–13Ta–4.6Zr. *Biomaterials* 2003;24:2673–2683.
24. Niinomi M, Hattori T, Morikawa K, Kasuga T, Suzuki A, Fukui H, et al. Development of low rigidity b-type titanium alloy for biomedical applications. *Mater Trans, JIM* 2002;43:2970–2977.
25. Lavos-Valereto IC, Konig B Jr, Rossa C Jr, Marcantonio E Jr, Zavaglia AC. A study of histological responses from Ti–6Al–7Nb alloy dental implants with and without plasma-sprayed hydroxyapatite coating in dogs. *J Mater Sci Mater Med* 2001;12:273–276.

26. Müller FA, Bottino MC, Müller L, Henriques VAR, Lohbauer U, Bressiani AHA, et al. In vitro apatite formation on chemically treated (P/M) Ti–13Nb–13Zr. *Dent Mater* 2008;24:50–56.
27. Okasaki Y, Gotoh E. Comparison of metal release from various metallic biomaterials in vivo. *Biomaterials* 2005;26:11–21.
28. Okasaki Y, Gotoh E, Manabe T, Kobayashi K. Comparison of metal concentrations in rat tibia tissues with various metallic implants. *Biomaterials* 2004;25:5913–5920.
29. Barril S, Mischler S, Landolt D. Influence of fretting regimes on the tribocorrosion behaviour of Ti6Al4V in 0.9 wt.% sodium chloride solution. *Wear* 2004;256:963-972.
30. Martin É, Azzi M, Salishchev GA, Szpunar J. Influence of microstructure and texture on the corrosion and tribocorrosion behavior of Ti–6Al–4V. *Tribol Int* 2010;43:918-924.
31. Sivakumar B, Kumar S, Sankara Narayanan TSN. Fretting corrosion behavior of Ti-6Al-4V alloy in artificial saliva containing varying concentrations of fluoride ions. *Wear* 2011;270:317-324.
32. Majumdar P, Singh SB, Chakraborty M. Wear response of heat-treated Ti–13Zr–13Nb alloy in dry condition and simulated body fluid. *Wear* 2008;264:1015-1025.
33. More NS, Diomidis N, Paul SN, Roy M, Mischler S. Tribocorrosion behavior of  $\beta$  titanium alloys in physiological solutions containing synovial components. *Mater Sci Eng C* 2011;31:400-408.

34. Choubey A, Basu B, Balasubramaniam R. Tribological behaviour of Ti-based alloys in simulated body fluid solution at fretting contacts. *Mater Sci Eng A* 2004;379:234-239.
35. Cvijović-Alagić I, Cvijović Z, Mitrović S, Panić V and Rakin M. Wear and corrosion behaviour of Ti–13Nb–13Zr and Ti–6Al–4V alloys in simulated physiological solution. *Corros Sci* 2011;53:796-808.
36. Tamilselvi S, Murugaraj R and Rajendran N. Electrochemical impedance spectroscopic studies of titanium and its alloys in saline medium. *Mater Corros* 2007;58:113-120.
37. Metikoš-Huković M, Kwokal A and Piljac J. The influence of niobium and vanadium on passivity of titanium-based implants in physiological solution. *Biomaterials* 2003;24:3765-3775.
38. Ask M, Lausmaa J, Kasemo B. Preparation and surface spectroscopic characterization of oxide films on Ti6Al4V. *Appl Surf Sci* 1989;35:283-301.
39. Yu SY, Scully JR, and Vitus CM. Influence of Niobium and Zirconium Alloying Additions on the Anodic Dissolution Behavior of Activated Titanium in HCl Solutions. *J Electrochem Soc* 2011;148:B68-B78.
40. Kubaschewski O, Hopkins BE. *Oxidation of metals*. London: Butterworths; 1962.
41. Elliott SR. *The physics and chemistry of solids*. Chichester. England: Wiley; 1998.
42. Ribeiro ALR, Caram Junior R, Cardoso FF, Fernandes Filho RB, Vaz LG. Mechanical, physical, and chemical characterization of Ti–35Nb–5Zr and



- Ti-35Nb-10Zr casting alloys. *J Mater Sci Mater Med* 2009;20:1629-1636.
43. Fusayama T, Katayori T, Nomoto S. Corrosion of gold and amalgam placed in contact with each other. *J Dent Res* 1963;42:1183-1197.
44. Li SJ, Yang R, Li S, Hao YL, Cui YY, Niinomi M, Guo ZX. Wear characteristics of Ti-Nb-Ta-Zr and Ti-6Al-4V alloys for biomedical applications. *Wear* 2004;257:869-876.
45. Mathew MT, Runa MJ, Laurent M, Jacobs JJ, Rocha LA, Wimmer MA. Tribocorrosion behavior of CoCrMo alloy for hip prosthesis as a function of loads: A comparison between two testing systems. *Wear* 2011;271:1210-1219.
46. Magaziner RS, Jain VK, Mall S. Investigation into wear of Ti-6Al-4V under reciprocating sliding conditions. *Wear* 2009;267:368-373.
47. Landolt D, Mischler S, Stemp M, Barril S. Third body effects and material fluxes in tribocorrosion systems involving a sliding contact. *Wear* 2004;256:517-524.

## **Considerações finais**

O objetivo central dessa tese foi investigar o comportamento eletroquímico e à tribocorrosão das novas ligas Ti35Nb5Zr e Ti35Nb10Zr para serem utilizadas como biomaterial na Odontologia, principalmente, na fabricação de implantes dentários e seus componentes, como substituintes da liga comercial mais utilizada Ti6Al4V. Em um estudo anterior, foi realizada a elaboração das ligas, caracterização das microestruturas e ensaios mecânicos<sup>68</sup>. Entretanto, não são conhecidas as propriedades dos seus filmes passivos que conferem proteção a corrosão e ao desgaste e, que agem diretamente na osseointegração. Portanto, levando em consideração o ambiente bucal agressivo, buscou-se compreender o comportamento dessas ligas frente a corrosão e tribocorrosão em saliva artificial a 37°C e compará-lo ao da liga Ti6Al4V.

O desenvolvimento do trabalho foi dividido em dois capítulos e nessa seção pretende-se interrelacionar os resultados encontrados. A metodologia da fundição das ligas e de todos os testes abordados na tese encontra-se detalhada no Apêndice.

### **Corrosão eletroquímica**

A corrosão eletroquímica das ligas de Ti está diretamente relacionada com as propriedades do filme passivo formado em suas superfícies.

Entende-se por filme passivo, a camada de óxidos que é formada na superfície dos metais, que confere proteção ao metal contra agentes externos<sup>8,21</sup>. Nos implantes e componentes protéticos dentários, o filme passivo do titânio e suas ligas é o que primeiro entra em contato com o ambiente bucal e osso. Portanto, se ele sofrer alteração, o metal base do sistema implante componente pode ficar exposto aos agentes

nocivos presentes na saliva artificial, aos esforços mecânicos, aos microorganismos e aos agentes de limpeza bucal.

O comportamento eletroquímico das ligas foi estudado por espectroscopia de impedância eletroquímica em função do tempo (0,5-216h), em potencial de circuito aberto. As três ligas apresentaram comportamento passivo quando imersas em saliva artificial, ou seja, formação de filme passivo. Entretanto a estrutura dos filmes foram diferentes. As ligas Ti6Al4V e Ti35Nb5Zr apresentaram filme duplo constituído por uma camada interna compacta e uma camada externa porosa. Já a camada de óxidos da liga Ti35Nb10Zr apresentou apenas a camada compacta.

Os principais óxidos formados na liga Ti6Al4V foram  $TiO_2$ ,  $Al_2O_3$  e  $VO_2$  sendo o óxido de Ti em maior concentração<sup>47,76</sup>. Nas ligas do sistema TiNbZr foram encontrados  $TiO_2$ ,  $Nb_2O_5$  e  $ZrO_2$ , sendo os óxidos de Ti e Nb em maior concentração, como verificado por Okasaki, Gotoh<sup>60</sup> e Yu et al.<sup>81</sup>. Sabe-se que o  $TiO_2$  apresenta bom comportamento eletroquímico<sup>8</sup> porém, a presença de  $Al_2O_3$ ,  $ZrO_2$ <sup>42,71</sup> e  $Nb_2O_5$ <sup>22,47,81</sup> na camada de óxidos de ligas de Ti proporciona aumento da resistência a corrosão. Entretanto a presença de  $VO_2$  é deletéria<sup>2,47,76</sup>.

As duas ligas de filme duplo apresentaram semelhante resistência a corrosão. Ao comparar as três ligas, a liga Ti35Nb10Zr obteve semelhante e melhor comportamento eletroquímico do que as ligas Ti35Nb5Zr e Ti6Al4V, respectivamente. Dessa forma, verificou-se que a quantidade de  $Nb_2O_5$  e  $ZrO_2$  presente na liga Ti35Nb10Zr foi suficiente para conferir a ela melhor comportamento quando comparada a liga Ti6Al4V.

## Tribocorrosão

A tribocorrosão é um processo de degradação resultante da ação simultânea de desgaste mecânico e corrosão eletroquímica na região de contato entre materiais que deslizam entre si, quando imersos em um meio agressivo<sup>36,50</sup>. No implantes dentários, a tribocorrosão pode estar presente entre as interfaces osso/implante, implante/componente protético e componente protético/prótese, devido aos micro-movimentos e ao ambiente agressivo.

Os testes de tribocorrosão foram realizados em circuito aberto com o tempo e em potencial anódico aplicado (500mV), em função da carga aplicada (50mN-1N).

Entre os resultados apresentados, destaque-se que as ligas do sistema TiNbZr apresentaram melhor comportamento tribocorrosivo quando foi aplicada carga de 50mN, não havendo mudança de potencial com o tempo nem sinal de desgaste, diferente do que ocorreu com a liga Ti6Al4V. Portanto, o filme passivo composto por  $TiO_2$ ,  $Nb_2O_5$  e  $ZrO_2$  foi mais resistente ao desgaste mecânico e a ação da saliva artificial. Entretanto, quando a carga aplicada foi superior a 80mN, o filme passivo de todas as ligas foi danificado, e o metal base sofreu desgaste mecânico.

Ao analisar as pistas de desgaste formadas após ensaio de tribocorrosão com carga de 1N, verificou-se que todas as pistas apresentavam características semelhantes de desgaste por abrasão<sup>18,52</sup>. Entretanto, na liga Ti6Al4V, a pista de desgaste formada foi mais estreita, provavelmente, relacionada com a maior dureza dessa metal, ou seja, maior resistência a deformação plástica<sup>45</sup>. Dessa forma, o comportamento do metal base dessa liga foi superior.

Além disso, no teste de tribocorrosão com potencial anódico aplicado com cargas aplicadas de 100mN, a liga Ti6Al4V também apresentou melhor resultado já que a quantidade de carga elétrica

liberada durante o deslizamento foi menor. Conseqüentemente, o metal base dessa liga obteve melhor resposta frente a tribocorrosão.

### **Corrosão x tribocorrosão**

A liga Ti35Nb10Zr obteve o melhor desempenho em relação a liga Ti6Al4V quando interrelacionados os testes de corrosão e de tribocorrosão com 50mN de carga aplicada devido principalmente a composição do seu filme passivo, que apresentou melhor resistência a corrosão e também ao desgaste.

O metal base da liga Ti6Al4V apresentou melhor comportamento tribocorrosivo, quando cargas superiores a 80mN foram aplicadas. Entretanto, sua menor resistência a corrosão é preocupante, pois íons podem ser liberados e prejudicar a saúde sistêmica dos pacientes.

Frente aos resultados apresentados, a liga Ti35Nb10Zr é promissora para ser utilizada na fabricação de implantes dentários. Vale ressaltar que ainda é preciso melhoria no processo de fabricação da liga para garantir maior homogeneidade. Para melhorar o comportamento tribocorrosivo, é sugerido realizar tratamentos de superfície como anodização, para que o filme passivo fique mais resistente aos esforços mecânicos. Ou ainda, realizar tratamentos térmicos para melhorar o comportamento do metal base frente ao processo de desgaste.

## Conclusão geral

As ligas Ti35Nb5Zr e Ti35Nb10Zr apresentaram superior comportamento tribocorrosivo em saliva artificial quando a carga aplicada foi 50mN. Ou seja, o filme passivo formado na superfície dessas ligas possuiu melhor comportamento eletroquímico e mecânico. Entretanto, a liga Ti35Nb10Zr apresentou maior resistência à corrosão que a liga Ti6Al4V, proporcionada pela quantidade de Nb<sub>2</sub>O<sub>5</sub> e ZrO<sub>2</sub> na composição do seu filme passivo.

A liga Ti6Al4V obteve melhor desempenho frente a tribocorrosão quando a carga aplicada era superior a 80mN devido ao melhor comportamento do seu metal base. Porém, a resistência a corrosão dessa liga foi inferior.

Diante dos resultados apresentados, a liga Ti35Nb10Zr é promissora para ser utilizada na fabricação de implantes dentários.

## Referências\*

1. Aleixo GT. Estabilidade e metaestabilidade de fases em ligas Ti-Nb [dissertação de mestrado]. Campinas: Faculdade de Engenharia Mecânica da UNICAMP; 2006.
2. Ask M, Lausmaa J, Kasemo B. Preparation and surface spectroscopic characterization of oxide films on Ti6Al4V. *Appl Surf Sci.* 1989; 35: 283-301.
3. ASM International Handbook Committee. ASM handbook. Ohio: ASM International; 1991. (v.4; Metals handbook: heat treating).
4. ASM International Handbook Committee. ASM handbook. Ohio: ASM International; 2004. (v.9; Metals handbook: metallography and microstructures).
5. Assem FL, Levy LS. A review of current toxicological concerns on vanadium pentoxide and other vanadium compounds: gaps in knowledge and directions for future research. *J Toxicol Environ Health B Crit Rev.* 2009; 12: 289-306.
6. Assis SL, Costa I. Electrochemical evaluation of Ti13Nb13Zr, Ti6Al4V and Ti6Al7Nb alloys for biomedical application by long-term immersion tests. *Mater Corros.* 2007; 58: 329-33.
7. Assis SL, Wolyneć S, Costa I. The electrochemical behaviour of Ti-13Nb13-Zr alloy in various solutions. *Mater Corros.* 2008; 59: 739-43.

---

\* De acordo com o estilo Vancouver. Disponível em:

[http://www.nlm.nih.gov/bsd/uniform\\_requirements.html](http://www.nlm.nih.gov/bsd/uniform_requirements.html)

8. Black J, Hasting G. Titanium and titanium alloys. In: Handbook of biomaterial properties. London: Springer-Verlag/Chapman & Hall; 1998. p. 590.
9. Bollen CM, Papaioanno W, Van Eldere J, Schepers E, Quirynen M, van Steenberghe D. The influence of abutment surface roughness on plaque accumulation and peri-implant mucositis. *Clin Oral Implants Res.* 1996; 7: 201-11.
10. Boyer R, Welsch G, Collings EW, editors. *Materials properties handbook: titanium alloys.* Ohio: ASM International; 1994.
11. Cai Z, Shafer T, Watanabe I, Nunn ME, Okabe T. Electrochemical characterization of cast titanium alloys. *Biomaterials.* 2003; 24: 213-8
12. Chang JC, Oshida Y, Gregory RL, Andres CJ, Barco TM, Brown DT. Electrochemical study on microbiology-related corrosion of metallic dental materials. *Biomed Mater Eng.* 2003; 13: 281-95.
13. Chaturvedi TP. An overview of the corrosion aspect of dental implants (titanium and its alloys). *Indian J Dent Res.* 2009; 20: 91-8.
14. Choubey A, Basu B, Balasubramaniam R. Tribological behaviour of Ti-based alloys in simulated body fluid solution at fretting contacts. *Mater Sci Eng A.* 2004; 379: 234-9.
15. Choubey A, Basu B, Balasubramaniam R. Electrochemical behaviour of ti-based alloys in simulated human body fluid environment. *Trends Biomater Artif Organs.* 2005; 18: 64-72.
16. Correa CB, Pires JR, Fernandes-Filho RB, Sartori R, Vaz LG. Fatigue and fluoride corrosion on *Streptococcus mutans* adherence to titanium-based implant/component surfaces. *J Prosthodont.* 2009; 18: 382-7.



17. Cremasco A, Messias AD, Esposito AR, Duek EADR, Caram R. Effects of alloying elements on the cytotoxic response of titanium alloys. *Mater Sci Eng C Mater Biol Appl.* 2011; 31: 833-9.
18. Cvijović-Alagić I, Cvijović Z, Mitrović S, Panić V, Rakin M. Wear and corrosion behaviour of Ti–13Nb–13Zr and Ti–6Al–4V alloys in simulated physiological solution. *Corr Sci.* 2011; 53: 796-808.
19. Dobromyslov AV, Elkin VA. Martensitic transformation and metastable  $\beta$ -phase in binary titanium alloys with d-metals of 4-6 periods. *Scr Mater.* 2001; 44: 905-10.
20. Domingo JL. Vanadium: a review of the reproductive and developmental toxicity. *Reprod Toxicol.* 1996; 10: 175-82.
21. Donachie Jr MJ. Titanium: a technical guide. Ohio: ASM International; 2000.
22. Elliott SR. The physics and chemistry of solids. Chichester, England: Wiley; 1998.
23. Fathi MH, Salehi M, Saatchi A, Mortazavi V, Moosavi SB. In vitro corrosion behavior of bioceramic, metallic, and bioceramic-metallic coated stainless steel dental implants. *Dent Mater.* 2003; 19: 188-98.
24. Fernandes AC, Vaz F, Ariza E, Rocha LA, Ribeiro ARL, Vieira AC, et al. Tribocorrosion behaviour of plasma nitrided and plasma nitrided + oxidised Ti6Al4V alloy. *Surf Coat Technol.* 2006; 200: 6218-24.

25. Freese HL, Volas MG, Wood R. Metallurgy and technological properties of titanium and titanium alloys. In: Brunette DM, Tengvall P, Textor M, Thomsen P. Titanium in medicine: material science, surface science, engineering, biological responses and medical applications. Berlin: Springer; 2001. p. 25-51.
26. Geetha M, Singh AK, Gogia AK., Asokamani R. Effect of thermomechanical processing on evolution of various phases in Ti-Nb-Zr alloys. *J Alloys Compd.* 2004; 384: 131-44.
27. Guo WY, Sun J, Wu JS. Electrochemical and XPS studies of corrosion behaviour of Ti-23Nb-0.7Ta-2Zr-O alloy in Ringer's solution. *Mater Chem Phys.* 2009; 113: 816-20.
28. Hon YH, Wang JY, Pan YN. Composition/phase structure and properties of titanium-niobium alloys. *Mater Trans.* 2003; 44: 2384-90.
29. Jones FH. Teeth and bones: applications of surface science to dental materials and related biomaterials. *Surf Sci Rep.* 2001; 42: 75-205.
30. Karasevskaya OP, Ivasishin OM, Semiatin SL, Matviychuk YV. Deformation behavior of beta-titanium alloys. *Mater Sci Eng A Struct Mater.* 2003; 354: 121-32.
31. Karov J, Hinberg I. Galvanic corrosion of selected dental alloys. *J Oral Rehabil.* 2001; 28: 212-9.
32. Khan MA, Williams RL, Williams DF. The corrosion behavior of Ti-6Al-4V, Ti-6Al-7Nb and Ti-13Nb-13Zr in protein solutions. *Biomaterials.* 1999; 20: 631-7.

33. Kim HS, Kim WY, Lim SH. Microstructure and elastic modulus of Ti-Nb-Si ternary alloys for biomedical applications. *Scr Mater.* 2006; 54: 887-91.
34. Kim JI, Kim HY, Inamura T, Hosoda H, Miyazaki S. Shape memory characteristics of Ti-22Nb-(2-8)Zr(at.%) biomedical alloys. *Mater Sci Eng A Struct Mater.* 2005; 403: 334-9.
35. Kobayashi E, Doi H, Yoneyama T, Hamanaka H, Gibson IR, Best SM et al. Influence of aging heat treatment on mechanical properties of biomedical Ti-Zr based ternary alloys containing niobium. *J Mater Sci Mater Med.* 1998; 9: 625-30.
36. Landolt D, Mischler S, Stemp M. Electrochemical methods in tribocorrosion: a critical appraisal. *Electrochim Acta.* 2001; 46: 3913-29.
37. Lee CM, Ju CP, Chern Lin, JH. Structure-property relationship of cast Ti-Nb alloys. *J Oral Rehabil.* 2002; 29: 314-22.
38. Lemire J, Appanna VD. Aluminum toxicity and astrocyte dysfunction: a metabolic link to neurological disorders. *J Inorg Biochem.* 2011; 105: 1513-7.
39. Leyens C, Peters M. Titanium and titanium alloys: fundamentals and applications. Koln: DLR – German Aerospace Center – Institute of Materials Research, Wiley – VCH, Koln, Germany; 2003.
40. Lindholm-Sethson B, Ardlin BI. Effects of pH and fluoride concentration on the corrosion of titanium. *J Biomed Mater Res A.* 2008; 86: 149-59.
41. Long M, Rack HJ. Friction and surface behavior of selected titanium alloys during reciprocating-sliding motion. *Wear.* 2001; 249: 158–68.

42. Lopez MF, Gutierrez A, Jimenez JA. Surface characterization of new non-toxic titanium alloys for use as biomaterials. *Surf Sci.* 2001; 482: 300-5.
43. Majumdar P, Singh SB, Chakraborty M. Wear response of heat-treated Ti–13Zr–13Nb alloy in dry condition and simulated body fluid. *Wear.* 2008; 264: 1015-25.
44. Marino CEB, Mascaro LH. EIS characterization of a Ti-dental implant in artificial saliva media: dissolution process of the oxide barrier. *J Electroanal Chem.* 2004; 568: 115-20.
45. Martin É, Azzi M, Salishchev GA, Szpunar J. Influence of microstructure and texture on the corrosion and tribocorrosion behavior of Ti–6Al–4V. *Tribol Int.* 2010; 43: 918-24.
46. Martins DQ. Efeito da adição de Zr no comportamento elástico de ligas Ti-Nb aplicadas em implantes ortopédicos [dissertação de mestrado]. Campinas: Faculdade de Engenharia Mecânica da UNICAMP; 2007.
47. Metikoš-Huković M, Kwokal A and Piljac J. The influence of niobium and vanadium on passivity of titanium-based implants in physiological solution. *Biomaterials.* 2003; 24: 3765-75.
48. Milosev I, Antolic V, Minovic A, Cor A, Herman S, Pavlovcic V, et al. Extensive metallosis and necrosis in failed prostheses with cemented titanium-alloy stems and ceramic heads. *J Bone Jt Surg Br.* 2000; 82: 352-7
49. Milosev I, Kosec T, Strehblow H-H. XPS and EIS study of the passive film formed on orthopaedic Ti-6Al-7Nb alloy in Hank's physiological solution. *Electrochem Acta.* 2008; 53: 3547-58.
50. Mischler S. Triboelectrochemical techniques and interpretation methods in tribocorrosion: a comparative evaluation. *Tribol Int.* 2008; 41: 573-83.

51. Molina C, Nogués L, Martínez-Gomis J, Peraire M, Salsench J, Sevilla P, et al. Dental casting alloys behaviour during power toothbrushing with toothpastes of various abrasivities. Part II: corrosion and ion release. *J Mater Sci Mater Med*. 2008; 19: 3015-9.
52. More NS, Diomidis N, Paul SN, Roy M, Mischler S. Tribocorrosion behavior of  $\beta$  titanium alloys in physiological solutions containing synovial components. *Mater Sci Eng C*. 2011; 31: 400-8.
53. Morgan TD, Wilson M. The effects of surface roughness and type of denture acrylic on biofilm formation by *Streptococcus oralis* in a constant depth film fermentor. *J Appl Microb*. 2001; 91: 47-53.
54. Ngwa HA, Kanthasamy A, Anantharam V, Song C, Witte T, Houk R, Kanthasamy AG. Vanadium induces dopaminergic neurotoxicity via protein kinase C $\delta$  dependent oxidative signaling mechanisms: Relevance to etiopathogenesis of Parkinson's disease. *Toxicol Appl Pharm*. 2009; 240: 273-85.
55. Niinomi M, Hattori T, Morikawa K, Kasuga T, Suzuki A, Fukui H, et al. Development of low rigidity  $\beta$ -type titanium alloy for biomedical applications. *Mater Trans*. 2002; 43: 2970-7.
56. Niinomi M. Fatigue performance and cyto-toxicity of low rigidity titanium alloy, Ti-29Nb-13Ta-4.6Zr. *Biomaterials*. 2003; 24: 2673-83.
57. Niinomi M. Mechanical biocompatibilities of titanium alloys for biomedical applications. *J Mech Behav Biomed Mater*. 2008; 1: 30-42.
58. Niinomi M. Mechanical properties of biomedical titanium alloys. *Mater Sci Eng A Struct Mater*. 1998; 243: 231-6.

59. Oh TJ, Yoon J, Misch CE, Wang HL. The causes of early implant bone loss: myth or science. *J Periodontol.* 2002; 73: 322-33.
60. Okasaki Y, Gotoh E. Comparison of metal release from various metallic biomaterials in vitro. *Biomaterials.* 2005; 26: 11-21.
61. Okazaki Y, Rao S, Asao S, Tateishi T, Katsuda S, Furuki Y. Effects of Ti, Al and V concentrations on cell viability. *Mater Trans, JIM.* 1998; 39: 1053-62.
62. Perl DP, Moalem S. Aluminum and Alzheimer's disease, a personal perspective after 25 years. *J Alzheimers Dis.* 2006; 9: 291-300.
63. Pipino F. The bone-prosthesis interaction. *J Orthopaed Traumatol.* 2000; 1: 3-9.
64. Ponthiaux P, Wenger F, Drees D, Celis JP. Electrochemical techniques for studying tribocorrosion processes. *Wear.* 2004; 256: 459-68.
65. Puleo DA, Nanci A. Understanding and controlling the bone-implant interface. *Biomaterials.* 1999; 20: 2311-21.
66. Rao S, Ushida T, Tateishi T, Okazaki Y, Asao S. Effect of Ti, Al, and V ions on the relative growth rate of fibroblasts (L929) and osteoblasts (MC3T3-E1) cells. *Biomed Mater Eng.* 1996; 6: 79-86.
67. Reclaru L, Meyer JM. Effects of fluorides on titanium and other dental alloys in dentistry. *Biomaterials.* 1998; 19: 85-92.
68. Ribeiro ALR, Caram Jr R, Cardoso FF, Fernandes Filho RB, Vaz LG. Mechanical, physical, and chemical characterization of Ti-35Nb-5Zr and Ti-35Nb-10Zr casting alloys. *J Mater Sci Mater Med.* 2009; 20: 1629-36.

69. Rimondini L, Farè S, Brambilla E, Felloni A, Consonni C, Brossa F, Carrassi A. The effect of surface roughness on early in vivo plaque colonization on titanium. *J Periodontol.* 1997; 68: 556-62.
70. Robin A, Carvalho OAS, Schneider SG, Schneider S. Corrosion behavior of Ti-xNb-13Zr alloys in Ringer's solution. *Mat Corr.* 2008; 59: 929-33.
71. Sahu S, Palaniappa M, Paul SN, Roy M. Potentiodynamic behaviour of Ti alloys in physiological solution containing lubricant. *Mater Lett.* 2010; 64: 2-14.
72. Scarano A, Piattelli M, Caputi S, Favero GA, Piattelli A. Bacterial adhesion on commercially pure titanium and zirconium oxide disks: an in vivo human study. *J Periodontol.* 2004; 75: 292-6.
73. Siddiqi A, Payne AG, De Silva RK, Duncan WJ. Titanium allergy: could it affect dental implant integration? *Clin Oral Implants Res.* 2011; 22: 673-80.
74. Souza MEP, Lima L, Lima CRP, Zavaglia CA, Freire CMA. Effects of pH on the electrochemical behaviour of titanium alloys for implant applications. *J Mater Sci Mater Med.* 2009; 20: 549-52.
75. Tang X, Ahmed T, Rack HJ. Phase transformations in Ti-Nb-Ta and Ti-Nb-Ta-Zr alloys. *J Mater Sci.* 2000; 35: 1805-11.
76. Tamilselvi S, Murugaraj R, Rajendran N. Electrochemical impedance spectroscopic studies of titanium and its alloys in saline medium. *Mater Corros.* 2007; 58: 113-20.
77. Urban RM, Jacobs JJ, Tomlinson MJ, Gavrilovic J, Black J, Peoc'h M. Dissemination of wear particles to the liver, spleen, and abdominal lymph nodes of patients with hip or knee replacement. *J Bone Joint Surg Am.* 2000; 82: 457-76.

78. Vieira AC, Ribeiro AR, Rocha LA, Celis AP. Influence of pH and corrosion inhibitors on the tribocorrosion of titanium in artificial saliva. *Wear*. 2006; 261: 994-1001.
79. Wang BL, Li L, Zheng YF. In vitro cytotoxicity and hemocompatibility studies of Ti-Nb, TiNbZr and Ti-Nb-Hf biomedical shape memory alloys. *Biomed Mater* [internet]. 2010; 5(4). Disponível em: [http://iopscience.iop.org/1748-605X/5/4/044102/pdf/1748-605X\\_5\\_4\\_044102.pdf](http://iopscience.iop.org/1748-605X/5/4/044102/pdf/1748-605X_5_4_044102.pdf)
80. Yang G, Zhang T. Phase transformation and mechanical properties of the  $Ti_{50}Zr_{30}Nb_{10}Ta_{10}$  alloy with low modulus and biocompatible. *J Alloys Compd*. 2005; 392: 291-4.
81. Yu SY, Scully JR, and Vitus CM. Influence of niobium and zirconium alloying additions on the anodic dissolution behavior of activated titanium in HCl solutions. *J Electrochem Soc*. 2001; 148: B68-B78.
82. Zavanelli RA, Guilherme AS, Pessanha-Henriques GE, Nóbilo MAA, Mesquita MF. Corrosion-fatigue of laser-repaired commercially pure titanium and Ti-6Al-4V alloy under different test environments. *J Oral Rehabil*. 2004; 31: 1029-34.
83. Zhou YL, Niinomi M, Akahori T, Fukui H, Toda H. Corrosion resistance and biocompatibility of Ti-Ta alloys for biomedical applications. *Mater Sci Eng A Struct Mater*. 2005; 398: 28-36.



## **Apêndice**

### **A1 Material e método**

#### **A1.1 Elaboração das ligas**

As ligas de Ti, Nb e Zr foram confeccionadas na forma de lingotes de aproximadamente 60g, com as composições: Ti35%Nb5%Zr e Ti35%Nb10%Zr (%m/m)<sup>6,7</sup>. Os lingotes foram fundidos em forno de fusão a arco-voltáico, com atmosfera inerte, controlada por bomba de vácuo e fluxo de argônio, alocado no Laboratório do Departamento de Física da Faculdade de Ciências de Bauru, UNESP, sob coordenação do Prof. Dr. Carlos Roberto Grandini. Os lingotes fundidos foram submetidos ao tratamento térmico de 1.000°C, por 8h, com controle da atmosfera, para promover a homogeneidade da estrutura metalúrgica. Em seguida, os lingotes foram forjados a quente em barras de 10mm e, em seguida, usinados na forma de discos (8mm de diâmetro x 8mm de altura). Na sequência, os discos foram submetidos ao segundo tratamento térmico de 1.000°C, por 1h, com resfriamento a ar, para aliviar as tensões geradas durante a usinagem.

A liga comercial Ti6Al4V foi adquirida em forma de cilindro e usinada em corpos-de-prova em forma de discos (25mm x 4,5mm).

#### **A1.2 Metodologia do Capítulo I**

##### **A1.2.1 Preparação das amostras**

Os discos foram polidos com lixas de carbetto de silício até uma granulometria de #1200 e então limpos em ultrassom, utilizando-se acetona (3min). Os discos foram então imersos em reagente de Kroll (1ml

de HF, 5ml de HNO<sub>3</sub>, 44ml de água destilada) por 10min. Em seguida, os discos foram limpos com propanol (10min) e água destilada a 60°C (15min) em ultrassom, e secados com ar quente. A limpeza com reagente de Kroll é realizada para a remoção total da camada de óxidos presente na superfície das ligas de Ti. Dessa forma, foi possível padronizar o tempo de crescimento do filme passivo nas diferentes ligas em 24h.

### A1.2.2 Análise das superfícies das ligas

A espectroscopia de Raios-X (XPS) foi realizada para analisar a composição do filme passivo das ligas de Ti, em dois momentos, 24h após a limpeza com reagente de Kroll e após 216h de imersão em solução de saliva artificial, similar à descrita por Fusayama et al.<sup>2</sup> (Quadro 1), com pH 5,25, a 37°C.

Quadro 1 - Composição química da saliva artificial (g/l)

NaCl	KCl	CaCl <sub>2</sub> .2H <sub>2</sub> O	Na <sub>2</sub> S.9H <sub>2</sub> O	NaH <sub>2</sub> PO <sub>4</sub> .2H <sub>2</sub> O	Uréia
0,4	0,4	0,795	0,005	0,69	1

O espectrômetro utilizado foi o UNI-SPECS UHV, do Departamento de Físico Química, IQ/UNESP, sob coordenação do Prof. Dr. Peter Hammer. A pressão base do sistema foi inferior a 10<sup>-7</sup>Pa. Foi utilizada a linha Mg K $\alpha$  (h $\nu$  = 1253,6eV) e a energia de passagem do analisador foi ajustada para 10eV. O ruído inelástico dos espectros foi subtraído utilizando-se o método de Shirley. A composição da camada da superfície foi determinada pelas proporções das áreas de picos corrigidas pelos fatores de sensibilidade (Scofield) dos elementos correspondentes. Os espectros foram desconvolucionados utilizando-se uma função do tipo Voigtiana, com combinações Gaussianas (70%) e Lorentzianas (30%). A largura à meia altura variou entre 1,1 e 2,1eV e a precisão na

determinação da composição variou  $\pm 10\%$ , e a posição dos picos foi determinada a uma precisão de  $\pm 0,1\text{eV}$ .

### **A1.2.3 Análises eletroquímicas**

Realizou-se curvas de polarização potenciodinâmicas, testes de potencial de circuito aberto com o tempo ( $E_{\text{corr}}$ ), e espectroscopia de impedância eletroquímica (EIS) com o intuito de verificar a estabilidade eletroquímica e a resistência à corrosão das três ligas em estudo, utilizando-se o potenciostato Reference 600, Gamry Instruments, Warminster, PA, EUA, do Laboratório de Caracterização de Materiais, Departamento de Engenharia Mecânica, Universidade do Minho, Portugal, sob coordenação do Prof. Luís Augusto Rocha

Os testes foram realizados em células eletroquímicas para três eletrodos, com O´ring de  $0,636\text{cm}^2$  de diâmetro quando os eletrodos de trabalho (ligas de titânio) eram expostos ao eletrólito. Os eletrodos de referência e auxiliar utilizados foram: o eletrodo de calomelano saturado (SCE) e eletrodo de platina, respectivamente. Todos os potenciais analisados tiveram como referência o SCE.

O eletrólito usado foi solução de saliva artificial (Quadro 1).

As curvas de polarização potenciodinâmicas, com faixa de potencial de  $-0,9$  a  $2\text{V}$  e velocidade de varredura de  $1\text{mV/s}$ , foram obtidas após  $216\text{h}$  em imersão em saliva artificial a  $37^\circ\text{C}$ . Foram determinados parâmetros, como a densidade de corrente de corrosão ( $i_{\text{corr}}$ ), que pode ser entendida como a velocidade de corrosão para um determinado potencial, e o potencial de corrosão ( $E_{(i=0)}$ ), que caracteriza a tendência do material para sofrer corrosão. Os resultados foram estatisticamente analisados pelo teste Kruskal-Wallis e pelo teste Dunn, para comparação dois a dois ( $\alpha=0,05$ ).

O  $E_{\text{corr}}$  foi monitorado durante  $216\text{h}$ , com o intuito de verificar a formação e a estabilidade do filme passivo das ligas em estudo.

Os parâmetros utilizados nos ensaios de EIS foram: frequência inicial 63kHz, frequência final 0,01Hz, velocidade de varredura 10mV/ms, em diferentes períodos de imersão em solução de saliva artificial (0,5h, 4h, 8h, 24h, 48h, 72h, 144h e 216h). A interpretação dos resultados foi realizada com o auxílio do programa Echem Analyst, do próprio potenciostato Gamry. Os resultados foram analisados estatisticamente pelo teste de análise de variância, seguido pelo teste de Tukey para comparação dois a dois, quando comparadas as três ligas, e quando comparadas duas ligas, foi utilizado o teste de Tukey ( $\alpha=0,05$ ).

Para cada situação estudada, os ensaios foram realizados em triplicata a fim de garantir reprodutibilidade.

### **A1.3 Metodologia do Capítulo II**

#### **A1.3.1 Dureza**

Para avaliar a dureza do material, os discos foram polidos com lixas de carbetto de silício até uma granulometria de #600 e então limpos em ultrassom utilizando-se acetona (3min), propanol (10min), água destilada (5min) e secados com ar quente.

Foram realizadas 12 análises de dureza Vickers, 500gf por 15s, em cada liga estudada. Utilizou-se o durômetro Micromet 2003, Buehler, do Departamento de Físico Química, IQ, UNESP. Os resultados foram analisados estatisticamente pelo teste de análise variância, seguido pelo teste de Tukey para comparação dois a dois.

#### **A1.3.2 Análise das superfícies**

As ligas de Ti foram analisadas por XPS conforme Capítulo 1.

### A1.3.3 Tribocorrosão

Os testes de tribocorrosão foram realizados em um tribômetro CETR (UMT-2, CETR, Campbell, California, USA), do Laboratório de Tribologia, Departamento de Engenharia Mecânica, Universidade do Minho, Portugal. Utilizou-se a configuração *ball-on-plate*, com esferas de alumina (quimicamente inerte) de 10mm de diâmetro como antagonista às três ligas em estudo, utilizando a técnica de deslizamento linear alternativo. O coeficiente de atrito foi monitorado durante os ensaios<sup>3,4</sup>.

Os experimentos foram realizados sob  $E_{\text{corr}}$  e também sob potencial anódico aplicado<sup>5</sup>, utilizando os mesmos eletrodos citados no Capítulo I. A célula eletroquímica utilizada nesse sistema não delimita a área exposta ao eletrólito. Portanto, foi utilizada cera de abelha para delimitar a área de exposição do metal em  $0,64\text{cm}^2$ . O eletrólito utilizado também foi a solução de saliva artificial citada anteriormente no Capítulo I (Quadro 1), a  $37^\circ\text{C}$ . Previamente aos testes de tribocorrosão, as amostras ficaram imersas em saliva artificial a  $37^\circ\text{C}$  e o  $E_{\text{corr}}$  foi monitorado para verificar o tempo de estabilização das ligas, estabelecido em 1200s no mínimo.

A Figura 1 mostra uma ilustração esquemática da configuração do teste de tribocorrosão. Como pode ser visto, um potenciostato está acoplado ao tribômetro, no qual uma célula de três eletrodos está posicionada, permitindo que ambos os parâmetros tribológicos e eletroquímicos pudessem ser mensurados simultaneamente.

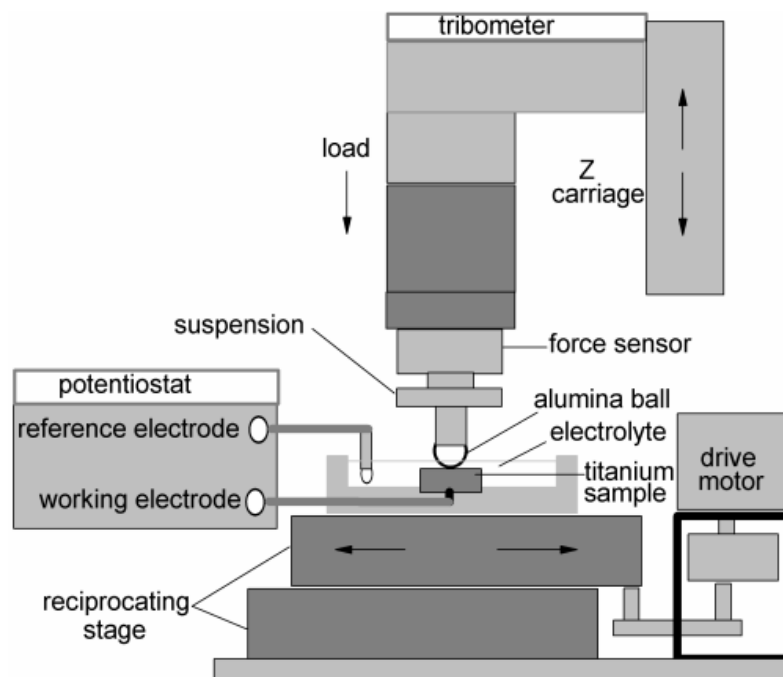


FIGURA 1 - Configuração da tribocorrosão<sup>1</sup>.

Nos testes de tribocorrosão sob  $E_{corr}$ , foram aplicadas diferentes cargas: 0,05N a 1N. Estabeleceu-se a amplitude de deslizamento de 5mm, frequência de 1Hz e tempo de ensaio igual a 1200s. A direção do deslizamento foi perpendicular aos riscos gerados no polimento.

O potencial escolhido para os testes de tribocorrosão, sob potencial anódico aplicado, foi 500mV vs. SCE, baseado nas curvas de polarização potenciodinâmicas (Figura 2). Esse valor representa um potencial passivo das três ligas em saliva artificial a 37°C. Os parâmetros utilizados para esses testes foram semelhantes aos citados anteriormente, porém, nesse caso, as cargas aplicadas foram 0,08N e 0,1N. O tempo de estabilização de corrente foi 500s antes e depois do deslizamento. A partir desses testes, foi possível analisar a quantidade de carga elétrica liberada durante o deslizamento pela integração das curvas

de corrente vs. tempo. Os resultados foram analisados estatisticamente pelo teste de análise de variância, seguido pelo teste de Tukey para comparação dois a dois ( $\alpha=0,05$ ).

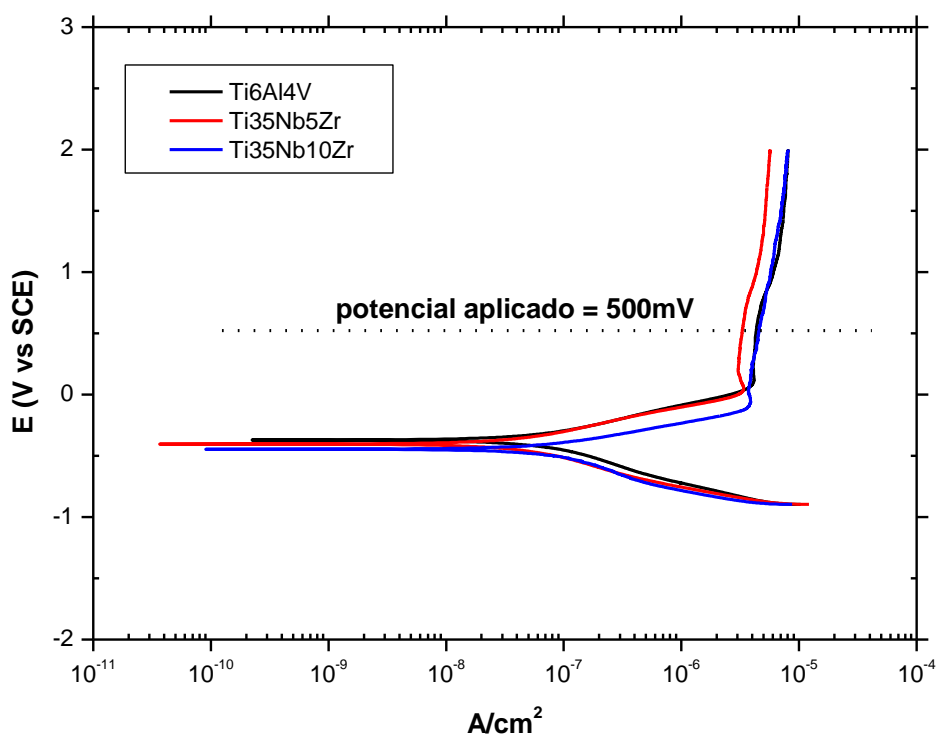


FIGURA 2 – Curvas de polarização potenciodinâmicas das ligas Ti6Al4V, Ti35Nb5Zr e Ti35Nb10Zr após 2h de imersão em saliva artificial a 37°C. Faixa de potencial de -0,9 a 2V e velocidade de varredura de 1mV/s.

Para cada situação estudada, os ensaios foram realizados em triplicata a fim de garantir reprodutibilidade.

As pistas de desgaste, obtidas após os testes de tribocorrosão, foram analisadas morfológicamente em um microscópio de alta resolução, Ultra-high resolution Field Emission Gun Scanning Electron Microscopy (FEG-SEM), NOVA 200 Nano SEM, FEI Company, e,

quimicamente por EDS, detector Si(Li), EDAX company, na Universidade do Minho, Portugal. As esferas de alumina foram analisadas para a verificação da transferência do metal, utilizando Microscópio Eletrônico de Varredura, Jeol-JSM, do Departamento de Físico Química, IQ, UNESP.

### Referências\*

1. Cruz HV, Souza JCM, Henriques M, Rocha LA. Tribocorrosion and bio-tribocorrosion in the oral environment: the case of dental implants. In: Davim JP. Biomedical Tribology. Aveiro: Nova Biomedical; 2011.
2. Fusayama T, Katayori T, Nomoto S. Corrosion of gold and amalgam placed in contact with each other. J Dent Res. 1963; 42: 1183-97.
3. Landolt D, Mischler S, Stemp M. Electrochemical methods in tribocorrosion: a critical appraisal. Electrochim Acta. 200; 46: 3913-29.
4. Mischler S. Triboelectrochemical techniques and interpretation methods in tribocorrosion: a comparative evaluation. Tribol Int. 2008; 41: 573-83.
5. Ponthiaux P, Wenger F, Drees D, Celis JP. Electrochemical techniques for studying tribocorrosion processes. Wear. 2004; 256: 459-68.

---

\* De acordo com o estilo Vancouver. Disponível em:

[http://www.nlm.nih.gov/bsd/uniform\\_requirements.html](http://www.nlm.nih.gov/bsd/uniform_requirements.html)



6. Ribeiro ALR. Caracterização mecânica, física e química das ligas Ti-35Nb-5Zr e Ti-35Nb-10Zr [dissertação de mestrado]. Araraquara: Faculdade de Odontologia da UNESP; 2008.
7. Ribeiro ALR, Caram Jr R, Cardoso FF, Fernandes Filho RB, Vaz LG. Mechanical, physical, and chemical characterization of Ti-35Nb-5Zr and Ti-35Nb-10Zr casting alloys. *J Mater Sci Mater Med*. 2009; 20: 1629-36.

Autorizo a reprodução deste trabalho.

(Direitos de publicação reservados ao autor)

Araraquara, 28 de março de 2012.

**ANA LÚCIA ROSELINO RIBEIRO**